Green facades for cooling urban hot spots

The cooling effectivity of green facades on spaces adjacent to and inside dwellings in Amsterdam

Florinde Vessies
Msc Thesis Metropolitan Analysis, Design and Engineering (MADE)
Wageningen University & TU Delft
August 2020

Green facades for cooling urban hot spots

The cooling effectivity of green facades on spaces adjacent to and inside dwellings in Amsterdam

By Florinde Vessies

In partial fulfilment of the requirements for the degree of

Master of Science in Metropolitan Analysis, Design and Engineering (Msc MADE)

August 8th, 2020

Supervised by
dr. ir. Marjolein Pijpers-van Esch, Urbanism, Technical University Delft
dr. ir. Bert van Hove, Meteorology and Air Quality, Wageningen University and Research
dr. ir. Cor Jacobs, Climate Resilience, Wageningen Environmental Research

Guidance was partly provided as part of the project "Effectief groen voor klimaatadaptatie in de stad". This project is financed by the top sector Tuinbouw & Uitgangsmaterialen, the OOGSt Fund, AMS Institute, VHG and ANTHOS.

AMSTERDAM INSTITUTE FOR ADVANCED METROPOLITAN SOLUTIONS

TU Delft

MSc MADE

WAGENINGEN UNIVERSITY & RESEARCH

ABSTRACT

To limit increasing heat problems in cities, green areas are being implemented in the urban context. Since space is often scarce in cities, an opportunity lies in the use of green facades. This research has investigated the cooling effect of natural green facades in the form of Hedera helix. Both the effect on thermal comfort inside and outside buildings was investigated during a five-day heatwave using a model approach in ENVI-met. For this purpose, energy labels and the urban heat island effect were used as heat exposure indicators to determine urban hot spots in Amsterdam. One study area was selected for which dwellings were simulated for four different orientations, namely facing north, east, south and west. The results demonstrated that green facades could account for small decreases (<1 °C) in air temperature and outdoor thermal comfort. This cooling effect was more pronounced for indoor temperatures, where the insulating function of the greening led to a maximum cooling of 3 °C for the southern oriented buildings within the first 24 hours. After a few days, the indoor effect appeared to fluctuate, namely resulting in lower temperatures during the night and higher temperatures during the day compared to a non-green facade. In conclusion, this research has demonstrated that green facades can reduce the heat accumulation of buildings as they function as an extra insulation layer. Further research may be necessary to determine which accompanying measures can optimize the cooling effect of green facades to limit urban heat problems.

ACKNOWLEDGEMENTS

I would like to express my gratitude to my supervisors Marjolein Pijpers-van Esch, Bert van Hove and Cor Jacobs for their guidance and support throughout my process. Their critical eye and constructive feedback have been extremely valuable.

In addition, I'd like to thank everybody that helped me shape this thesis in identifying research gaps, creating context on the subject, and providing technical support in their free time: Laura Kleerekoper, Marc Ottelé, Daan Verhorst and Corné Vreugdenhil. Also, I would like to sincerely thank Stan Putman and Hester de Vries for their diligent proofreading of this thesis.

Furthermore, I want to express my gratitude to my parents for supporting me throughout my studies and for lending me their kitchen table during the lockdown; I don't think I'll ever have an office with such a large desk again. Also, I'd like to thank my friends and Teisse: your support has served me very well in this process.

Florinde Vessies,

Amsterdam, August 2020

TABLE OF CONTENTS

LIST OF FIGURES

LIST OF TABLES

ACRONYMS AND TERMINOLOGY

Term/abbreviation	Definition
PET	Physical equivalent temperature (°C)
T_{mrt}	Mean radiant temperature (°C). The uniform temperature of an imaginary enclosure (or environment) in which radiant heat transfer from the human body is equal to the radiant heat transfer in the actual nonuniform enclosure (or environment)
T_a	Air temperature (°C)
q	relative concentration of water vapour, expressed as specific humidity (kg/kg)
v	Wind velocity (m/s)
Heat flux	The flow of heat per unit area (W/m2)
Energy balance	Mathematical model that includes the major flows of energy into and out of an ecosystem
Leaf Area Index	The amount of leaf surface area per unit of wall or ground area (m2/m2)
Latent energy	Energy required to change the phase of water from liquid to vapor.
Evaporative cooling	Process by which a liquid absorbs energy when it is evaporated
UCL	Urban Canopy Layer
UBL	Urban Boundary Layer
Potential air temperature	Potential air temperature at reference (and model default) pressure in ENVI-met. For the 3D model, it can be treated like the absolute air temperature
Stomatal Resistance	Actual resistance of stomata to vapour transfer (s/m)
Direct Shortwave radiation	Available direct solar radiation upon a reference surface perpendicular to the incoming sun rays (W/m2). May also be computed for a horizontal surface.
Diffuse Shortwave Radiation	Available diffuse solar radiation referring to a horizontal reference surface (W/m2)
Leaf Area Density (LAD)	The total one-sided leaf area per unit volume

1. INTRODUCTION

Climate change and urban heat

As a result of climate change, temperatures are expected to rise all over the world. Depending on the prediction model, an increase of 2°C to 3-4°C degrees is expected (IPCC, 2013). For the Netherlands, the KNMI developed four climate scenarios, wherein all scenarios an increase in average air temperatures are predicted. The number of heatwaves is expected to increase and also the heatwaves are expected to last longer, possibly with triple the number of hot days with a minimum of 25 °C in 2050 (KNMI, 2015). Moreover, according to Barriopedro et al. (2011) also the occurrence of 'mega-heatwaves', which stand out from typical heatwaves due to their large spatial extension, intensity, and persistence, might increase with 5 to 10 percent. Warming is especially a concern in cities due to the increasing urbanisation in relation to the Urban Heat Island (UHI) effect, due to which urban areas remain warmer than their surrounding hinterlands (Oke, 1982). Because of this effect, in addition to high temperatures in the city, heat stress exposure for residents is expected to increase substantially (Molenaar et al., 2016). The heat harms humans, for example by disrupting sleep, physiological and health problems or even death (Kenney et al., 2014; Klok & Kluck, 2018).

While buildings on the one hand can reduce the exposure to heat by providing a cool indoor climate, research has shown that climate change can cause overheating to occur more frequently and stay on for longer periods in many Dutch buildings (van Hooff et al., 2014). With high thermal resistance that prevents the loss of heat and large windows that admit sunlight, buildings in the Netherlands are historically mainly prepared for generating a comfortable indoor climate during cold periods (Kleerekoper, 2017). However, with higher outdoor temperatures and no passive cooling systems, this can cause overheating of Dutch dwellings. Without an increase in air conditioning many houses will be prone to more days with high temperatures indoors, which can lead to unfavourable situations due to heat stress.

Combatting urban heat - the potential of facade greening

Cooling mechanisms are thus required to mitigate heat issues. As green areas in cities are known to decrease air temperature, they are often opted for as adaptation strategy. However, due to the lack of space in cities, it is often difficult to realize an increase in green spaces. An opportunity may lie in the use of green facades, to which all kinds of positive effects are attributed: they may lower the outdoor temperature, take away air pollutants, increase biodiversity, make streets more attractive and have a positive effect on the well-being of citizens (Francis & Lorimer, 2011; Jänicke et al., 2015; Ostendorf et al., 2011). To tackle the heat problem in cities, green facades are thus expected to provide a viable solution. However, it is still unclear to what extent green facades could contribute to cooling in Dutch cities.

The heat reduction by facade greening can occur by providing shadow, evaporation and insulation (Perez et al., 2011). In terms of insulation, green facades significantly decrease the heat transfer if placed on a wall in comparison with a non-green wall. The interception of direct sunlight by plants thereby decreases indoor temperatures (Krusche et al., 1982). Outdoors green facades can lead to significant decreases in air temperatures close to buildings: Cameron, Taylor and Emmett (2014) showed air temperature differences of 3 °C during daytime in the air adjacent to vegetated walls compared to non-vegetated walls at an 8 cm distance. In the majority of literature the focus however lies on the effect on the surface temperatures of buildings, where the plant cover leads to reduced wall temperatures compared to bare facades (Alexandri & Jones, 2004; Hoelscher et al., 2016). However, air temperature alone is not an accurate indicator of how humans experience heat or cold stress. A better indicator is the thermal comfort, which explains the sense of satisfaction humans have with the thermal environment. Thermal comfort depends on a combination of air temperature, mean radiant temperature, humidity and wind velocity and tends to show larger differences than air temperatures (Höppe, 1999). The Physiological Equivalent Temperature (PET) is one of the indices of thermal comfort and is weighted to the human perception of climate circumstances, such as metabolic rate and physical work output. In cities, large variations in thermal comfort can occur due to spatial and temporal differences in neighbourhood properties. Additionally, the impact of green facades shows a seasonal variation and depends on the amount and geometry of the vegetation, the species used and the climate (Alexandri & Jones, 2004). As a result, the cooling effects of green facades reported in scientific literature cannot be translated directly into the Dutch context.

Problem statement

The growing heat problem in Dutch cities has gained more attention during the past years (Klok et al., 2019; Kluck et al., 2020; Rovers et al., 2014). Although several mitigation strategies have been researched, the cooling effect of green facades has only been linked to the Dutch climate in a handful of occasions (Kluck et al., 2020; Ottelé, 2011). Literature on green facades is rarely focused on streets or neighbourhoods that are most exposed to heat and could thus benefit from this heat mitigation strategy. Likewise, it is still unknown how the building features and orientation influence the potential cooling effect. Evidence of the cooling effect of green facades on outdoor temperatures, thermal comfort and indoor air temperatures in Dutch cities is thus lacking. Moreover, most research on green facades runs for short periods without addressing the accumulation of heat in buildings during heatwaves (Taleghani et al., 2014; Wilschut et al., 2019). Lastly, indoor and outdoor temperatures have rarely been studied simultaneously and if so, only in an experimental set up (Hoelscher et al., 2016). So far, no scientific modelling research exists that considers the impact of green facades on indoor and outdoor temperatures simultaneously for the Dutch climate. In this master thesis the impact of green facades on the indoor and outdoor urban microclimate during a heatwave will therefore be assessed using a modelling approach.

Research objective

This research aims to investigate the effect of green facades on thermal comfort inside and outside buildings. It also seeks to determine the most problematic heat areas in Amsterdam. Using a case study, a model approach is subsequently used to determine the effect of the green facade on the urban microclimate in Amsterdam. This will be investigated by means of the following research question:

How do natural green facades affect the indoor and outdoor thermal comfort of dwellings in the urban microclimate in Amsterdam?

This research question will be answered through addressing the following sub-research questions:

Sub question 1:

For which areas in Amsterdam are green facades relevant in terms of decreasing the indoor and outdoor temperatures?

Sub question 2: Outdoor

a. What is the effect of green facades and dwelling orientation on air temperature?

b. What is the effect of green facades and dwelling orientation on thermal comfort, measured in PET?

Sub question 3: Indoor

What is the effect of green facades and dwelling orientation on the inside air temperatures of dwellings?

2. THEORETICAL FRAMEWORK

This chapter describes the theoretical background and context of the research. Firstly, the urban climate and urban energy balance will be explained to show the context behind this research. Secondly, the energy exchange of buildings will be outlined, followed by a description of the relationship between indoor and outdoor temperatures. Lastly, green facades are introduced and their function and impact on temperatures will be explained.

2. 1. Urban climate

Global warming is causing an increase in heatwaves and hot nights in the Netherlands. The KNMI has therefore drawn up four climate scenarios, considering a moderate to warm scenario for the global average temperature and a low to high value for the change in atmospheric circulation. Outcomes of these scenarios all predict an increase in the average temperature (KNMI, 2015). Urban areas are additionally exposed to different temperatures than the rural hinterlands. In cities it is generally warmer than in surrounding areas due to climate change in combination with the Urban Heat Island (UHI) effect, which means that urban areas are more prone to experiencing extremely high temperatures than the surrounding rural area. The UHI effect has several causes, such as the heat absorption by paved and impermeable surfaces, the lack of vegetation in cities, the waste heat generated by energy sources. This difference between rural hinterlands and cities are found to be 8 °C or more for Dutch cities (Van Hove et al., 2011).

Two different types of UHI are distinguished:

- The surface UHI – The surface temperature difference between urban areas and rural hinterlands
- The atmospheric UHI – The air temperature difference between urban areas and rural hinterlands, where the atmospheric UHI can be broken down into two components:
    - The UHI in the atmospheric boundary layer, of which the intensity depends on the morphology, general configuration and geographic locati on of the city
    - Urban Canopy Layer UHI, which affects the urban microclimate. Here the presence of buildings, street surface, trees and water directly influence the microclimatic conditions and living environment

Oke (1976) distinguished that the atmospheric heat islands are recognized based on two layers of the atmosphere: the Urban Canopy Layer, that entails the layers from ground to roof level and covers the processes that are controlled by microscale, site-specific characteristics and

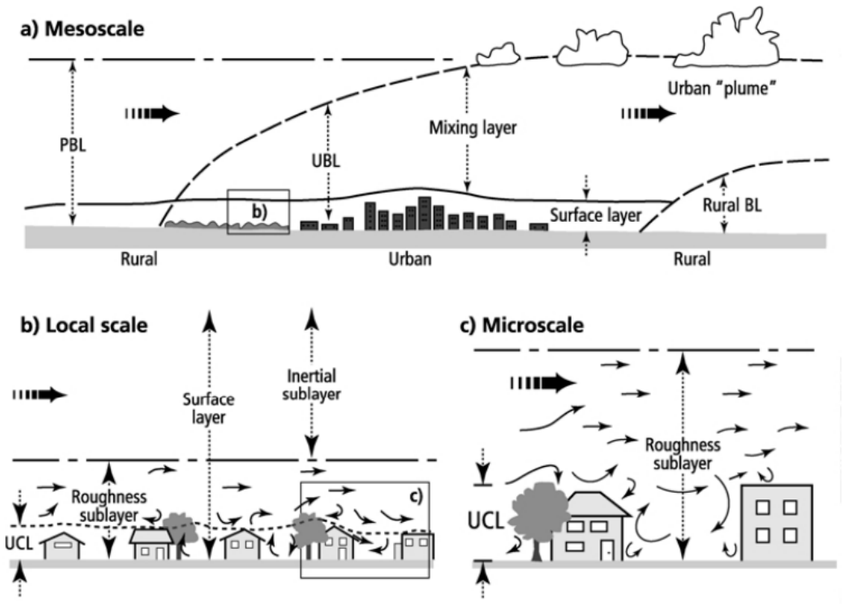

Figure 1 The city scales and its vertical layers with in a. the mesoscale of the city with Planetary Boundary Layer (PBL) and Urban Boundary Layer (UBL), in b. the local scale interactions with the Urban Canopy Layer (UCL) and in c. The microscale on street level and interactions with the UCL. Figure derived from Piringer et al. (2002) based on the original of Oke (1976).

processes, such as airflow and the energy exchange, and the Urban Boundary Layer (Figure 1). The UBL is a local to mesoscale phenomenon that occurs above roof level and entails processes operating at larger spatial and temporal scales, which are affected by the urban surface and airflow below. The UCL, on the other hand, is a microscale to describe properties of air between buildings and is directly affected by nature and surroundings.

Surface UHI is most pronounced during the day and shortly after sunset. Maximum temperatures are reached during the daytime when surfaces absorb solar radiation. In a comparative study across 419 cities, a negative correlation was found between the day time surface UHI and the difference of vegetation cover between urban and suburban areas (Peng et al., 2012). This suggests that increasing the urban vegetation cover could be an effective way to mitigate the Surface UHI effect. Atmospheric UHIs however become more apparent after sunset due to the slow release of heat from the urban area. The peak of heat release depends on the urban and rural surfaces, the season and weather conditions (Van Hove et al., 2011). At night air and surface temperatures are more similar than during the day due to still-warm urban surfaces losing heat to the air that is blocked by the buildings in the area. The diurnal patterns of surface and air temperature differences are visualised in Figure 2. The focus of this research lies in the atmospheric UHI on the level of the UCL and its interaction with the urban microclimate, as this has the largest effect on humans in the living environment.

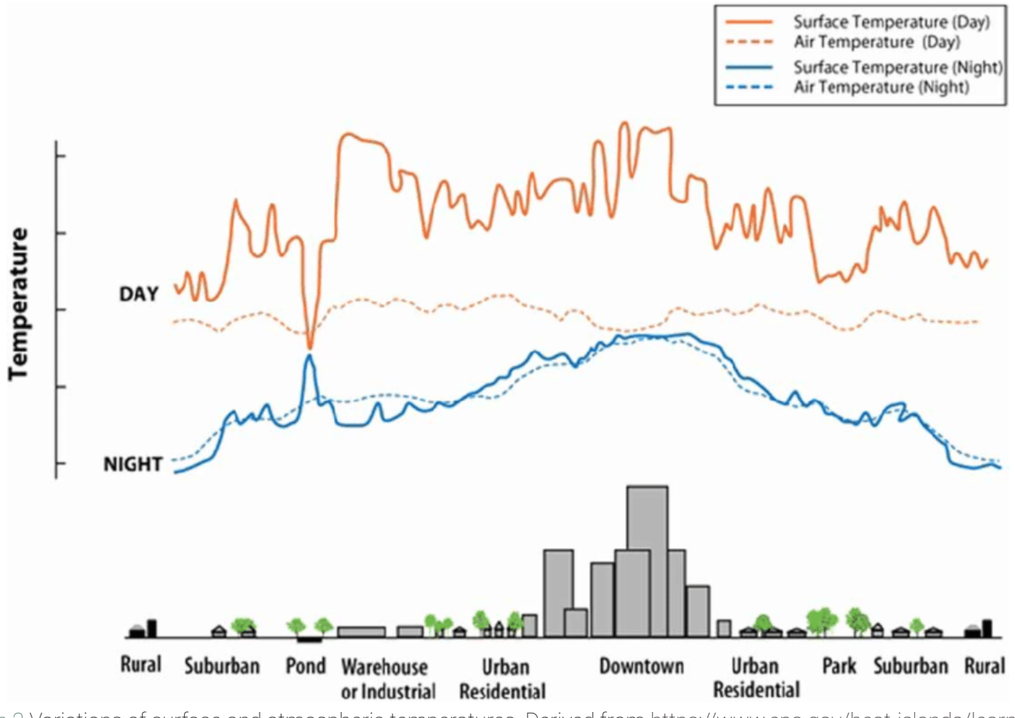

Figure 2 Variations of surface and atmospheric temperatures. Derived from https://www.epa.gov/heat-islands/learn-about-heat-islands

2. 2. The urban energy balance

An explanation of the UHI effect lies in the energy balance of urban areas. This energy balance is significantly different from rural areas due to differences in land cover, surface characteristics and level of human activity (Oke, 1982; Van Hove et al., 2011). When using a volume approach, the urban surface energy balance reads (Figure 3):

$$Q^* + Q_f = Q_h + Q_e + \Delta Q_s + \Delta Q_a \quad (1)$$

Where Q^* is the net radiation (the sum of net short-wave radiation and net long-wave radiation), Q_f is the anthropogenic heat release from the urban area, Q_h is the turbulent sensible heat flux, Q_e is the turbulent latent heat flux from evapotranspiration. ΔQ_s refers to the net storage heat flux and ΔQ_a is the net advection flux.

Each component of the energy balance can be altered in the urban environment and thus contribute to the UHI (Oke, 1988). Four parameters that are directly relevant to heat islands are surface albedo, evapotranspiration from vegetation, the anthropogenic heating from mobile and stationary sources and the sky view factor (Taha, 1997). The albedo of a surface is its absorption of shortwave radiation. The lower the albedo, the more radiation is absorbed, often leading to higher surface temperatures. In cities, pavement, stones and other impervious surfaces absorb more heat in comparison to rural areas. As the net available energy is distributed, this means that increased evaporation and transpiration through plants results in a decrease in remaining energy for the sensible heat flux (Q_e). In cities, the evapotranspiration rate is lower than in rural areas due to the sealed soils by pavement, leading to an increase in night-time temperatures. The anthropogenic heat represents all the heat released by human-induced processes, such as heating and cooling, running appliances, transportation and industrial processes. In addition, the sky view factor helps

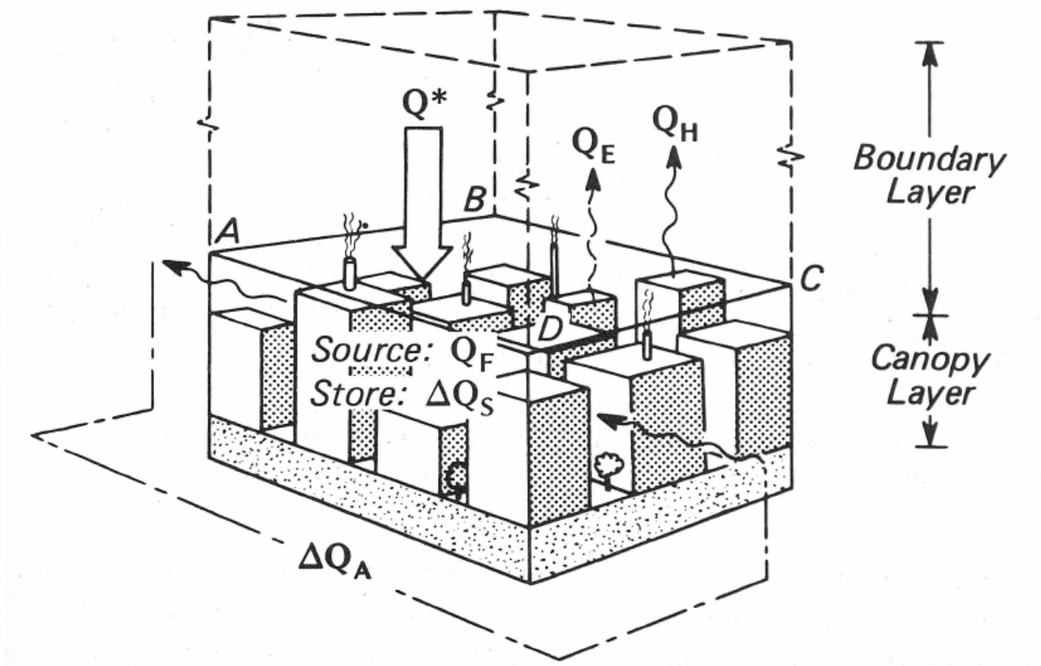

Figure 3 the energic basis of the Urban Heat Island effect. From Oke, T. R. (1988). The urban energy balance. Progress in Physical Geography, 12(4), 471–508.

to describe the urban climatology and its spatial variations, which is an indicator of the street geometry and building density (Dirksen et al., 2019). The obstruction of the sky by buildings in the city results in decreased long-wave radiative heat loss out of street canyons and reduced turbulent heat transport due to building height, roughness and orientation. This leads to an increased net heat storage within buildings and an increase of the UHI.

2. 3. Thermodynamics of buildings

The building is a complex thermodynamic system, with both internal and external heat sources that all can affect the indoor air temperature. The boundaries of the building's thermodynamic system are known as the building's envelope, which consists of walls, windows, floors, roofs and the chimney. All the different materials of the building envelope, the outdoor climatic factors and the users affect the energy budget and the temperatures in buildings (Sadineni et al., 2011). The heat balance (or energy balance) of the building depends on the heat transmission, incoming solar radiation, internal heat load and energy needs of the building. Differences in air ventilation and infiltration (incoming or outgoing air) can lead to a loss or gain in the perceptible heat. A schematic representation of the different flows of thermal energy in and out of a building is given in Figure 4.

Essential for this research is the role of the wall in the energy exchange. The thermal resistance (RC value) of the wall is crucial as it strongly influences the building energy consumption. This RC value measures the effectiveness of insulation, where a higher number represents more effective insulation and thus a reduced heat flux through the wall. The use of green facades can increase the RC value by about 25% and thus have positive implications on the thermal properties of buildings (Pan & Xiao, 2014).

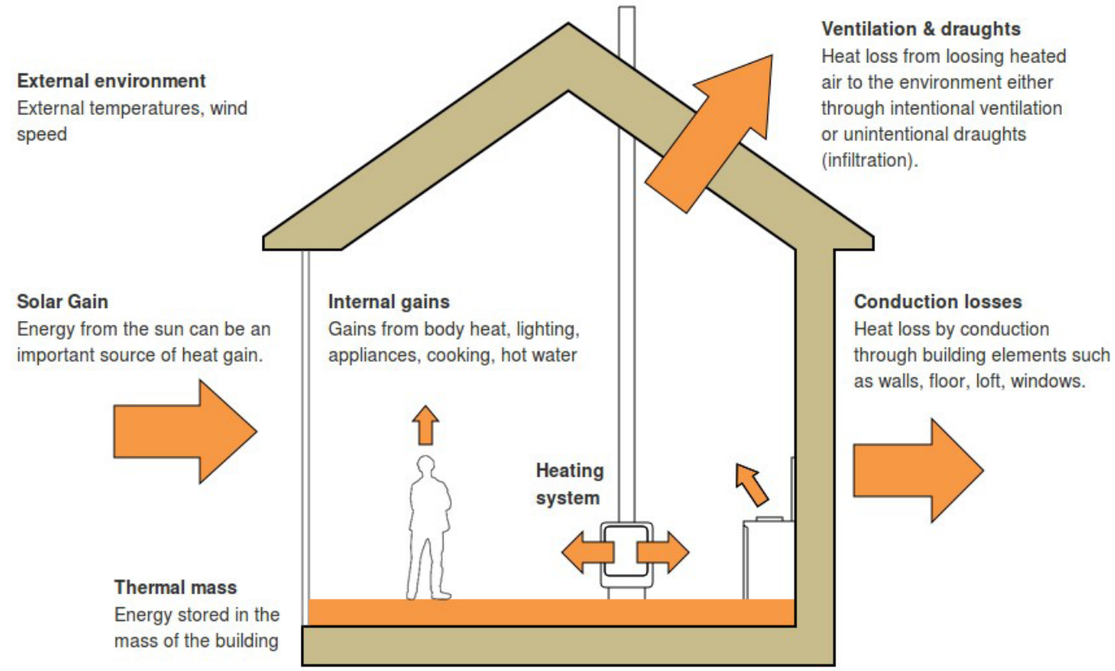

Figure 4 Energy exchange in buildings. Figure derived from https://learn.openenergymonitor.org/sustainable-energy/building-energy-model/readme

2. 3. 1. Energy labels

Since the 1990s a commonly used measure of the thermal performance of buildings are energy labels.This energy certification for buildings emerged intending to reduce energy consumption without compromising comfort, health and productivity levels. In the Netherlands, the energy label is based on the 'Degree on Energy Performance of Buildings' (in Dutch 'Besluit Energieprestatie Gebouwen' (BEG)) and the 'Regulation on Energy Performance of Buildings' (in Dutch 'Regeling Energieprestatie Gebouwen' (REG), which are both based on the Energy Performance of Buildings Directive regulations (EPBD) (ISSO, 2009). The objective of the labels is to make residents and homeowners aware of the thermal quality of their homes. Although energy labels could be based on technical simulations, they typically rely on the expected (theoretical) energy usage, expressed in kWh electricity, m3 gas and GJ heat (Majcen et al., 2013). The labels rely on the energy index formula that entails the total energy consumption:

$$Qtotal = Q\ space\ heating + Qwater\ heating + Qaux.energy + Qlighting - Qpv - Qcogeneration \quad (2)$$

Consisting of heating, hot water, pumps/ventilators and lighting, minus the energy gains from potential PV cells and/or cogeneration. To make the energy labels of different buildings comparable, *Qtotal* is corrected for the floor area and the corresponding heat transmission areas and is based on average occupancy and the average outdoor climate. The lifestyle and behaviour of occupants is not included. Buildings are classified on a scale, varying from A++ to G using an energy labelling index. The relationship between the energy labels and the energy index values can be found in Table 1.

Energy label	Corresponding Energy Index
A++	<0.5
A+	0.51-0.70
A	0.71-1.05
B	1.06-1.30
C	1.31-1.60
D	1.61-2.00
E	2.01-2.40
F	2.41-2.90
G	>2.9

Table 1 Dutch energy labels and the corresponding energy values (Huurcommissie, 2019)

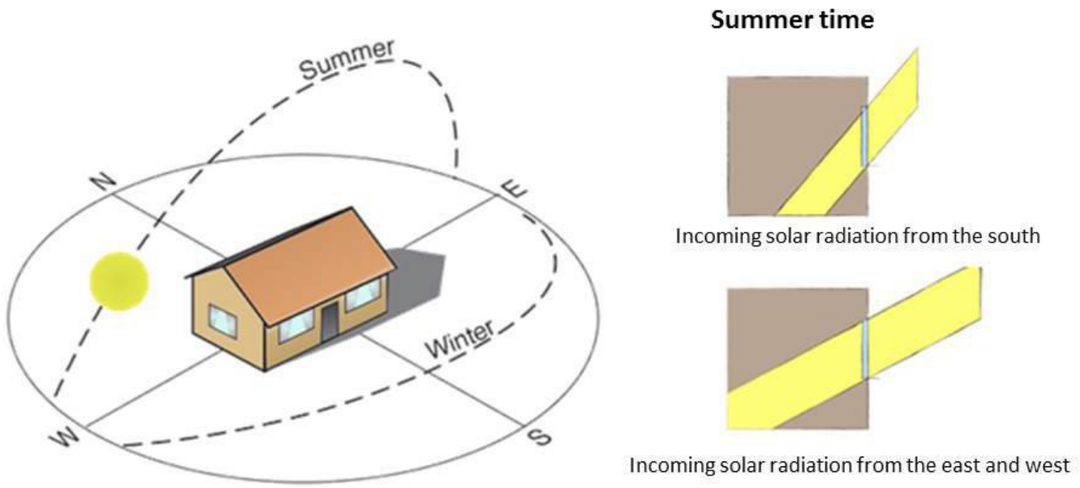

Figure 5 Overview of the sun's path in summer and winter. The figure on the right shows solar radiation received by the windows on the south compared to the windows on the east and west (Rovers et al., 2014).

The energy labels of buildings and thus their thermal performance can identify where people potentially experience the greatest heat stress. Van Hooff et al. (2014) showed that buildings with lower insulation values generally experience fewer overheating hours during the year than buildings with higher thermal resistance. This seems counterintuitive but can be explained by the reduced heat transport through the envelope. Once the air inside the building has been heated by solar radiation it cools down much slower. However, the research by van Hooff et al. (2014) did not assess peak temperatures and heat stress during those moments.

2. 3. 2. Orientation

The amount of solar radiation that reaches the building envelope can influence the energy balance drastically. Large amounts of solar radiation can lead to a large incoming heat load into a building, which can lead to high indoor temperatures. In the middle of summer, the sun rises in the north east and sets in the north west, which means that the northern facade receives solar radiation in the early morning and late evening. Although north oriented windows remain coolest, this leads to a larger energy demand in winter as the solar heat yield is minimal. Due to the solar inclination and azimuth angle (solar direction) windows facing east and west will receive larger amount of solar radiation in summer, inducing higher indoor temperatures than windows facing north and south (Figure 5). In winter however, the solar gain through east or west windows is lower, as the sun sets before the solar radiation reaches the windows (Andersson et al., 1985). This can cause higher heating costs in winter for dwellings with windows facing east or west than the southern orientation because incoming solar heat equals the loss, whilst surplus heat is generated in summer. The optimal orientation in terms of energy consumption and solar transmittance are therefore south oriented buildings, followed by the east, west and north oriented buildings.

Several studies have investigated the relationship between indoor and outdoor temperatures (Nguyen et al., 2014; Quinn et al., 2014). Nguyen et al. (2014) found wthat the relationship between indoor and outdoor temperature is nonlinear: with high outdoor temperatures a strong correlation with indoor temperature was found, but this correlation was weak for lower outdoor temperatures. In temperate climates, higher outdoor temperatures thus lead to high indoor temperatures, while low outdoor temperatures do not automatically result in low in-house temperatures.

Other aspects that influence the indoor temperatures were researched by Tamerius et al. (2013). In an experiment in 327 dwellings in New York City, they discovered that the type of building and the floor of the house significantly affect the indoor temperature, despite similar outdoor air temperatures. Interior surfaces such as walls, roofs and thermal mass can influence the energy exchange between inside and outside areas together with the radiative and thermal properties of construction materials and the orientation wof the building. Indoor air temperatures as experienced by humans thus depend on multiple factors.

2. 3. 3. Outdoor thermal comfort

Air temperature alone is not a comprehensive measure of outdoor thermal comfort as other aspects such as wind speed, air humidity and mean radiant temperature have to be taken into account as well (Lin & Matzarakis, 2008). A measure of outdoor thermal comfort is the thermal index of Physiological Equivalent Temperature (PET), which is derived from the human energy balance equation (Höppe, 1999):

$$M + W + R + C + E_D + E_{Re} + E_{Sw} + S = 0 \quad (3)$$

Where M is the metabolic rate of the body, W the physical work output, R the net radiation of the body, C the convective heat flow, E_D the imperceptible perspiration (latent heat flow related to evaporation of water diffusing through the skin), E_{Re} the sum of heat flows for heating and humidifying the inspired air, E_{Sw} the heat flow due to evaporation of sweat and S the storage heat flow for heating or cooling the body mass. The heat flows (C, E_d, E_{Re}, E_{sw} and S) are all expressed in Watt. Meteorological parameters influence these individual heat flows: E_{Re} and C are controlled by air temperature, E_D, E_{Re} and E_{Sw} by the air humidity, C and E_{Sw} by the wind velocity and the net radiation of the body (R) by the mean radiant temperature (Höppe, 1999). In addition, the heat resistance of clothing (clo) and activity of humans (W)

are accounted for. The body's response to air temperature is influenced by the integrated effect of all meteorological parameters that interact with each other.

The PET is defined as the air temperature at which, in a typical indoor setting (without wind and solar radiation), the heat budget of the human body (a standardized person) is balanced with the same core and skin temperature as in the complex outdoor conditions. This helps to compare the integral effects of complex thermal conditions in different situations including indoors. The reference indoor environment is defined by the mean radiant temperature equalling the air temperature, having a constant air velocity of 0.1 m/s and a water vapour pressure of 12 hPa. The standardized person used in this setting is characterized by a work metabolism of 80 W of a light activity on top of the basic metabolism, and a heat resistance of 0.9 clo as a result of clothing. Matzarakis & Mayer (1996) described how PET relates to thermal perception and the grade of physiological stress (Table 2).

In this research PET will be used to assess thermal comfort outdoors, while the interior air temperature will be used as an indicator of indoor thermal comfort.

2. 3. 4. Influence of green facades

Green facades have cooling effects through transpiration and shading and among others can affect the surface temperature of buildings and air temperature. In terms of outdoor temperatures Cameron, Taylor and Emmett (2014) showed outdoor air temperature differences of 3 °C during daytime in air adjacent to vegetated walls compared to non-vegetated walls at an 8 cm distance, while a 5 °C difference at 50 cm from the wall was found by (Djedjig et al., 2015). This cooling effect has been observed particularly at surface temperatures in previous research. As the plant covers the bare facade, the wall heats up at a reduced rate, which can result in a reduction of more than 10 degrees of the surface temperature of the facade (Alexandri & Jones, 2004; Hoelscher et al., 2016). Larger coverage of the facade with a thick foliar layer can lead to a larger cooling effect.

Green facades can affect indoor temperatures by functioning as an extra insulation layer through exterior temperature regulation. This insulating effect is brought about by the stagnant air layer that exists between the building and the vertical green layer which slows down the rate of heat transfer between the interior and exterior of a building (Krusche, von Lersner, & Otto, 1982, as cited in Ottelé, 2011). The insulation value of a building's facade can be increased in several ways. Firstly, covering the facade with vegetation prevents heat to reach the buildings surface in summers. In winters the extra insulation layer prevents the internal heat from escaping. Secondly, the plant layer can act as a buffer that keeps wind from moving along a buildings surface (Peck et al., 1999). Additional ways in which green facades affect indoor temperatures are the interception of direct sunlight by plants and reduced heating or even cooling of the air by evaporation (Perez et al., 2011). In summer, these factors can reduce indoor temperatures, but the degree to which this cooling occurs depends on the type of green facade (Hoelscher et al., 2016).

Perez et al. (2011) proposed an overarching name of all facade greening systems currently available: green vertical systems of buildings. These consist of green facades and living walls. Living walls consist of panels or geotextile felts that are built on vertical support. Green facades are systems consisting of climbing plants or hanging port shrubs together with a support structure. Plants can either be planted directly into the ground or in pots. Green facade systems can be subdivided into three different categories: traditional green facades, where facade material is used as support for climbing plants, double-skin green facade or

PET °C	Thermal perception	Grade of physiological stress
< 4	Very cold	Extreme cold stress
4 – 8	Cold	Strong cold stress
8 – 13	Cool	Moderate cold stress
13 – 18	Slightly cool	Slight cold stress
18 – 23	Comfortable	No thermal stress
23 – 29	Slightly warm	Slight heat stress
29 – 35	Warm	Moderate heat stress
35 – 41	Hot	Strong heat stress
> 41	Very hot	Extreme heat stress

Table 2 PET classes, thermal perception and grade of physiological stress (Andreas Matzarakis & Mayer, 1996)

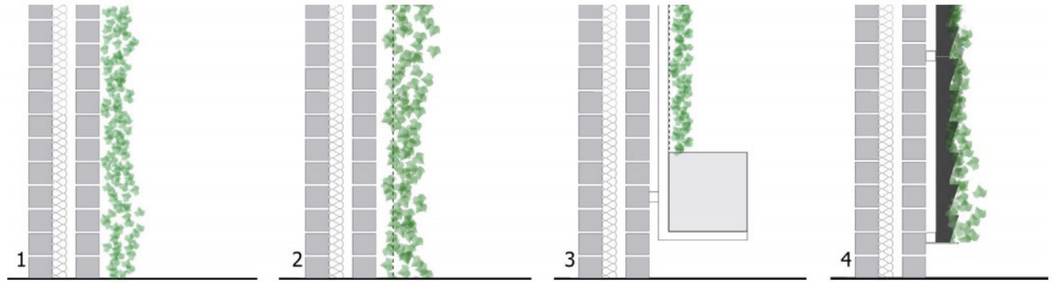

Figure 6 Examples of vertical greening systems with in 1. Direct green facade, 2. Indirect green facade, 3. Indirect green facade combined with planter boxes and in 4. Living wall system (Perini & Rosasco, 2013)

Advantages	Disadvantages
• Low planting costsSuitable for retrofit projects • Relatively little technical expertise needed • Increased biodiversity development • Breeding and nesting possibilities • No need for irrigation systems • Reduction of indoor and outdoor temperature due to evapotranspiration and shadowing • Conversion of air polluting • Substances (CO2, NOx and SO2) • Adsorption of particulate matter (PMx) on leaves • Improved aesthetic value	• Chance on moisture problems (construction without a cavity wall) • Maintenance costs • Not suitable for each construction • Long growing period to get result • Maximum greening height of +/- 25 meters

Table 3 Advantages and disadvantages of direct green facades by Ottelé (2011)

green curtain, where the plants are separated from the wall in order to create a double-skin and perimeter flower pots, where hanging port shrubs are planted around the building to build up a green facade. Examples of these four categories of green vertical systems are given in Figure 6. This research focuses on traditional green facades that are directly placed on the wall (Figure 6.1). The advantages and disadvantage of this type of green facades have been reviewed by (Ottelé, 2011) and are shown in Table 3.

Different species vary in their cooling capacity due to their differences in geometry and leaf density, soil moisture, the climate and the season. As different species have different leaf area indices (the total one□ sided area of leaf tissue per unit ground surface area), stomatal resistance (the opposition to transport water vapor and carbon dioxide to or from the stomata on the leaves of plants) and transpiration, this can influence the heat energy absorption and heat flux through the wall. In an experimental set up, Hoelscher et al. (2016) compared three types of climbing plants on facades in Germany: Parthenocissus tricuspidata, Hedera helix and Fallopia baldschuanica. All species significantly reduced the surface temperatures of the outside walls, by at least 12 degrees, and for the interior wall up to 1.7 degrees Celsius during night-time. Cameron et al. (2014) furthermore identified that the greatest cooling of wall temperatures was reached by Hedera helix a and Stachys byzantina, as these species formed a denser canopy on the wall. The mechanisms for providing air and wall cooling varied between species. Their results also indicated that Fuchsia promoted cooling of surface temperatures by evapotranspiration, whereas shade cooling resulted from was more important in Jasminum and Lonicera.

3. METHODOLOGY

Figure 7 shows the general design of the study. Three successive steps can be distinguished. First, the exposure of urban areas to heat stress was mapped. With this map a study area was selected. Finally, the model simulation study was performed for the selected urban areas in which the impact of green facades on outdoor and indoor temperatures was assessed.

Figure 7 Overview of the workflow

3. 1. Study area selection through exposure analysis in ArcGIS Pro

A spatial exposure analysis was carried out to determine where heat risks can occur for residents of Amsterdam. Risk here is determined by the climate and weather events (the hazards) in combination with the exposure and vulnerability to these hazards (Cardona, 2011; IPCC, 2012). Hazards refer to the possible future occurrences of (heat) events that may have adverse effects on vulnerable and exposed elements, such as humans (Birkmann, 2006). Exposure concerns the inventory of elements in an area where hazards might take place (UNISDR, 2004). This means that without population or economic resources exposed to potentially dangerous settings, no risk would exist. Vulnerability here refers to the propensity

of exposed elements (such as human beings) to suffer from hazard events, mostly in terms of social and environmental processes (Birkmann, 2006; Janssen et al., 2006). Vulnerability is situation-specific and directly related to the susceptibility, sensitivity and lack of resilience of the exposed system to adapt to hazards and exposures. The relationship between risk, hazard, vulnerability and exposure is visualized in Figure 8.

Within the context of this study, a hazard can be seen as a heatwave, the exposure as the places in the city where indoor and outdoor temperatures are most likely to rise, and the vulnerability as the social, economic and psychological characteristics of the population that makes them more prone to heat. Since the focus of this research concerns the possible cooling effect of green facades, an exposure analysis was carried out for Amsterdam. As the vulnerability and heat experience of the inhabitants do not fall within the scope of the research, they were not further examined.

Two heat exposure indicators are used in this research, namely UHI as outdoor factor and energy labels as indoor factor. Large temperature increases in cities due to the UHI indicate which locations in cities are prone to outdoor heat stress. As low energy labels indicate low thermal resistance - and hence accelerated warming of buildings - this is used as an indicator of increased indoor heat exposure.

Additional selection criteria were focused on the possible implementation of green facades. For two reasons, only buildings of housing corporations are included in this investigation. Firstly, Runhaar et al., (2012) showed that housing corporations did not pay much attention to heat stress in the past. Many housing associations agreed to retrofit their building stock to an average energy performance label of B as soon as possible, continuing to label A in 2030 and energy neutral by 2050 (Sociaal-Economische Raad, 2013). Many dwellings of the social housing stock however are still waiting to be upgraded. Secondly, decisions to renovate are made by the housing corporation for several buildings at the same time. This implies that, if green facades reduce the inside air temperatures significantly, implementation could be performed on a larger scale. Dwellings with a monumental status were excluded from the selection, since municipal policy prohibits application of green facades to such dwellings (Gemeente Amsterdam, 2016).

A spatial representation in the form of maps of the energy labels of housing corporation

Figure 8 Risk is defined as a combination of hazard, vulnerability and exposure.

dwellings and UHI values was gathered of Amsterdam. A spatial exposure assessment was carried out with these heat stress indicators using a weighted overlay in the latest version of geographical information system ArcGIS Pro (2.5.0). The analysis overlays several maps using a common measurement scale and weighs each of the indicators according to its importance. All buildings of housing corporations obtained a value based on exposure, where high values indicated high exposure and low values low exposure. A spatial Hot Spot Analysis (Getis-Ord Gi*) using the values of the weighted overlay analysis was carried out to determine where exposed clusters existed. This tool calculates the z-scores and p-values that indicate where high or low values cluster spatially. High z-scores and small p-values indicated spatial clustering of high values – low z-scores and low p-values identified cold spots. In this research only hot spots were taken into consideration. A confidence interval of 95 percent was used in this research. The resulting hot spot map identified the clusters that were most exposed to heat, indicated by the UHI and energy labels. Based on data availability and current knowledge on renovations of corporate-owned buildings, one housing block was selected as study area.

3. 2. Modelling exposed heat areas in ENVI-met

To assess the impact of green facades on the selected exposed study area in Amsterdam, the selected dwellings and its surroundings were simulated with ENVI-met V4.4. This model is a three-dimensional micro-scale model based on a computational fluid dynamic approach to simulate surface-vegetation-atmosphere interactions (M. Bruse, 2000; M. Bruse & Fleer, 1998). Output variables are air temperature, humidity, wind speed, wind direction, average radiation temperature and other meteorological parameters for the urban microclimate environment. In addition, it takes the physiological processes of vegetation into account, while giving a very detailed representation of this vegetation (Skelhorn et al., 2014). It is able to simulate green wall and roof performances as a solution to sustainable urban development (D. Bruse, 2018). Figure 9 shows the workflow of the simulation model, consisting of the model preparation, justification of grid size and model output.

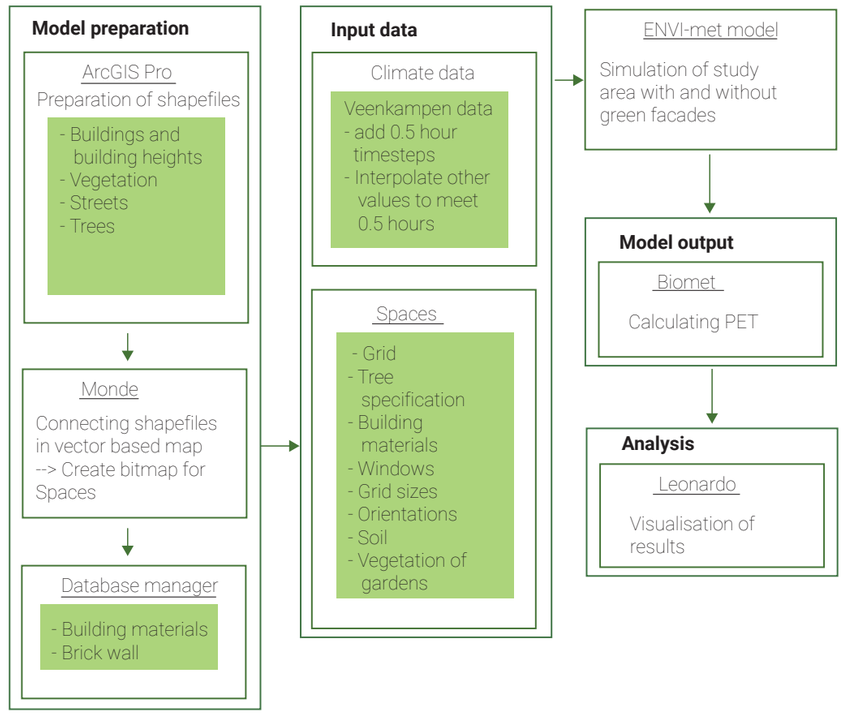

Figure 9 Flow chart of the preparation and executing of the modelling approach

3. 2. 1. Set up of the simulations

To model the microclimate at the selected location, shapefiles of buildings, trees, pavement and vegetation were prepared in ArcGIS Pro, in order to create a vector-based map that could be converted to a grid-based model area (Appendix B). In Spaces, the software to create the model area, specific properties of the study area such as building materials and windows were applied. Wall materials that resembled the walls of the study area were prepared in the Database Manager of ENVI-met. In combination with selected weather data, these were used as input for simulations.

The study area was simulated for five consecutive days during a heatwave in the summer of 2018. The area was simulated both with and without green facades to identify the potential differences. To identify the effect of building orientation on thermal comfort and the cooling capabilities of green facades, the study area was simulated in four different orientations: north, east, south and west.

3. 2. 2. Justification of grid and study area size

The size of the grid cell can have a significant influence on the results of the simulations (Kleerekoper, 2017). Through the grid-based model of Spaces and ENVI-met, all simulated factors are computed per grid cell. The size of the grid cell can range between 0.5x0.5 meter and 10x10 meter. Although higher resolutions generate the most accurate results, it is not necessarily the most favourable option as these simulations can be highly time intensive. In an effort to solve this optimization problem, we looked for a trade-off that would produce a reliable result with the shortest computation time possible. To do so a sensitivity analysis was performed for both grid size and study area size.

3. 2. 3. Model output

Three variables were selected to assess the impact of green facades. To determine the effect indoors, the indoor air temperature was used, which is output from ENVI-met. Outdoor effects of orientations and green facades were tested using two parameters: air temperature and PET, the used measure of thermal comfort. The potential air temperature output of ENVI-met was used as air temperature parameter, as this approximately equals the air temperature near the surface. Throughout the rest of this thesis it will be referred to as air temperature. PET values were calculated using Biomet, a postprocessing tool provided with the ENVI-met software. All values were evaluated directly in front of the facade and averaged over 6 grid cells using RStudio. Spatial patterns were compared using the visualisation software Leonardo provided with ENVI-met. Variations throughout the full simulation period for the different parameters were examined using Microsoft Excel.

4. DEFINING HEAT-EXPOSED AREAS IN AMSTERDAM

This section identifies the areas in Amsterdam that are most exposed to heat based on the energy labels of dwellings and the UHI-effect. Afterwards the study area specifics and model input for ENVI-met are elaborated upon.

4. 1. Exposed hot spots of housing corporation buildings

4. 1. 1. Exposure indicators

Energy labels

The energy labels of buildings and thus its thermal performance can identify which dwellings in the city are most exposed to heat and where green facades could have the biggest impact on indoor temperatures by functioning as an extra insulation layer. This extra insulation layer can, especially when used in combination with other heat mitigation measures such as sun blinds or triple layered glass, result in slower heat accumulation in buildings. Based on the energy index formula in (2),

$$Qtotal = Q\ space\ heating + Qwater\ heating + Q\ aux.energy + Qlighting - Qpv - Qcogeneration \quad (2)$$

this implies a lower *Qspace heating*, resulting in a lower *Qtotal*. This impact will be largest for dwellings with low energy labels, since there are still many opportunities there to reduce the *Qtotal*. In summer this would mean that the heat transfer from outdoor to the indoor climate happens at a reduced rate. while in winter the heating warmth can be captured for a longer period. Therefore, in this research, dwellings with low energy labels are seen as most exposed to heat.

ArcGIS Pro was used to map the different energy labels throughout Amsterdam. The energy labelling database from 'Energielabels Corporatiewoningen' of the ministry of Economic Affairs and Climate Policy was used, in which the energy labels of the national buildings stock of housing corporations are captured for the year 2017. These data points were combined with the vector data of buildings from the Basisregistratie Adressen en Gebouwen (BAG) of the Netherlands. However, since there are many dwellings with several addresses within the same building in Amsterdam and the facades of multiple floors will be greened, the average of energy labels per building was calculated to have one energy label for the entire building. Energy labels were translated into values from 1 to 7, where 1 resembled A (highest value in the database) and 7 G (lowest possible value). An overview of the spatial distribution of energy labels is visualised in Figure 10.

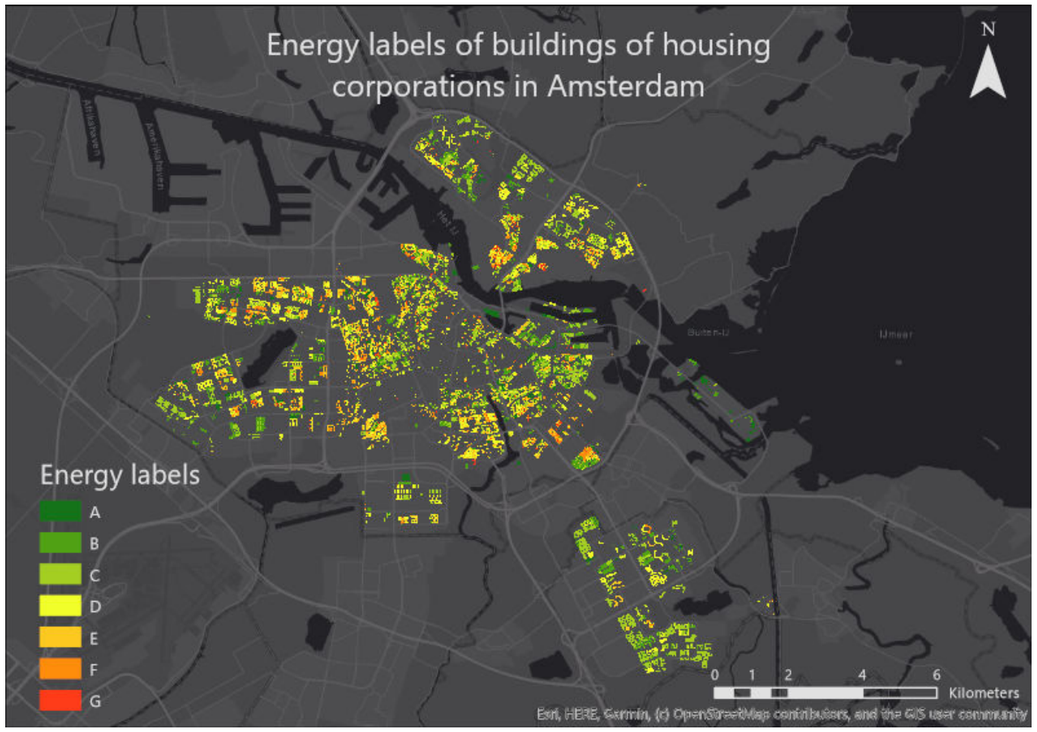

Figure 10 Average energy labels of buildings of housing corporations in Amsterdam

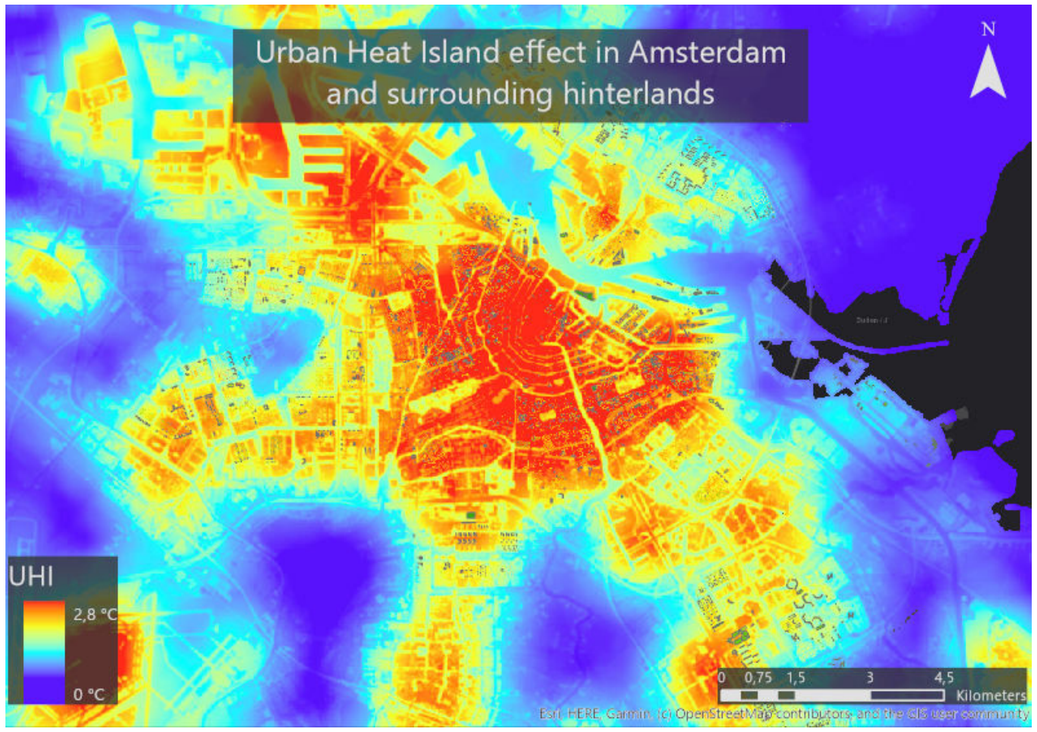

Figure 11 Spatial differences in UHI temperatures in Amsterdam and surrounding hinterlands

Urban Heat Island Effect

The heat problems occurring in cities are often linked to the UHI-effect. The maximum UHI is usually measured after sunset when the heat stored in roads, buildings and other structures during daytime is released again. It is however not the sole cause of these heat issues: the UHI is a contributing factor to hot weather and causes of the number of summer and tropical days and nights in addition to the changes induced by climate change.

So, UHI intensity gives an incomplete representation of thermal comfort and heat stress in cities. Nevertheless, it does identify areas that can get hotter than other areas of the city. As such, assessing UHI strengths helps to identify buildings in the city that are most exposed to heat, both indoors and outdoors. To this end, it was decided to use the UHI map of Atlas Natuurlijk Kapitaal (RIVM, 2018). The map from the RIVM is based on research by Lauwaet et al. (2015) and calculates the UHI on city level based on two factors: the population density in the city (and on a 10km radius around the city) and wind speed at 10 meters above land surface. Green areas on a local scale have an extra cooling effect. In addition, the cooling effects green and blue areas (such as forests, parks and ponds) are taken into account: if green and blue are present, the maximum UHI will be reduced within a 1-kilometer radius. For smaller, local green patches the actual UHI per location is estimated in a radius of 30 meter around a green. Based on these factors, the RIVM determines the maximum UHI in the city. The map shows annual averages, leading to a maximum UHI of 3°C. The UHI however can be a lot more pronounced on hot summer days. Figure 11 shows the UHI differences between Amsterdam and its hinterlands.

4. 2. Hot spot analysis in ArcGIS

A spatial weighted overlay was used to select areas for green facades using two criteria. To perform a weighted overlay the data on energy labels were converted to raster data. The data of the UHI effect were reclassified into 10 equally distributed groups, numbered between 1-10, where 1 was the coolest and 10 the hottest. The energy labels were used as integers with values from 1 – 7, where 1 resembled label A and 7 G. Both criteria were assigned the same weights (50%) in the analysis. Exposure values represented by the model's output were classified on a scale from 1-9, where 1 represented the locations least exposed to heat, and 9 the most exposed areas. In Figure 12 the normal distribution of the outcome values is shown.

These assigned exposure values of all buildings of housing corporations were then used in a cluster analysis to identify where statistically significant hot spots occurred with exposed dwellings. This was of interest to enable the possible widespread implementation of green facades at street or neighbourhood level based on the results. The hot spot analysis indicated where the observed spatial clustering of high values is more pronounced than one would expect in a random distribution of those same values. In this analysis a 95 percent confidence interval was used. In the cluster identification, the spatial relationships among the exposure feature were specified by the inverse distance, meaning that nearby neighbouring features had a larger influence on the computations for a target feature than features further away. The distance was calculated using a Euclidean distance with a threshold of 30 meters, as this could identify buildings in the same street. Several neighbourhoods contain hot spots of dwellings in the 95-confidence interval. The distribution throughout the city is visualized in Figure 13.

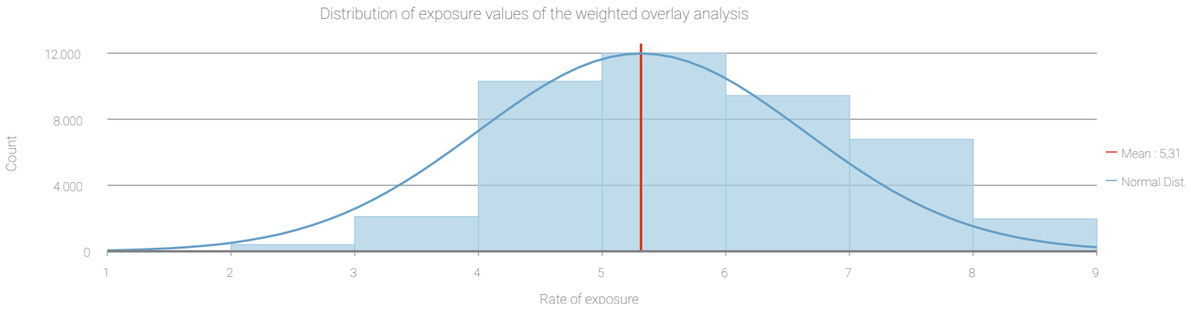

Figure 12 Distribution of exposure values, where 1 indicates the least exposed areas and 9 the most exposed sections

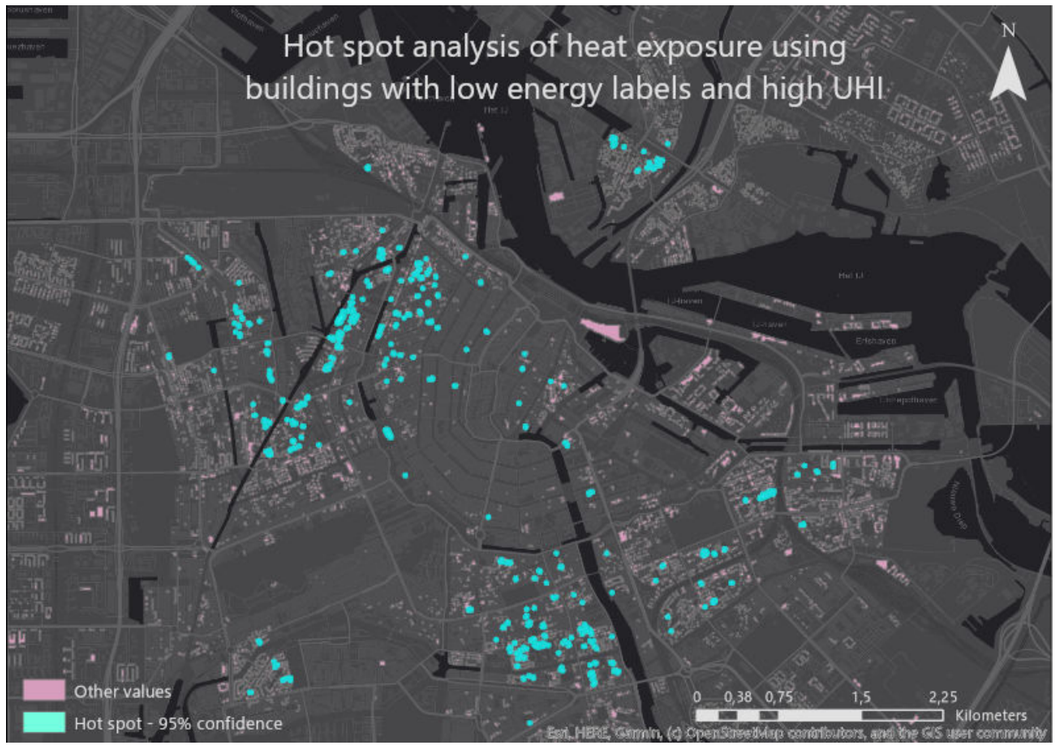

Figure 13 Spatial representation of hot spots of most exposed heat areas in Amsterdam based on energy labels and UHI

4. 2. 1. Identified hot spot neighbourhoods in Amsterdam

Several neighbourhoods contained hot spots of heat exposure. To make the results of the study implementable for different buildings, it was decided to select a district containing several buildings from the group of most exposed dwellings. Several neighbourhoods contained hot spot clusters: The Van der Pek neighbourhood in Amsterdam Noord, the Marathonbuurt and Diamantbuurt in Amsterdam Zuid, parts of the Dapperbuurt in Amsterdam Oost and the Frederik Hendrikbuurt in Amsterdam West (Figure 14).

a. Tweede van Swindenstraat in the Dapperbuurt

b. Rombout Hogerbeetsstraat in the Frederik Hendrikbuurt

c. Hygiëastraat in the Marathonbuurt

d. Saffierstraat in the Diamantbuurt

Figure 14 Identified hot spots in Amsterdam. All pictures derived from https://maps.google.com/

e. Gentiaanplein in the Van der Pekbuurt

Except for the Van der Pekbuurt, all neighbourhoods consist of four-story buildings in building blocks with numerous large windows on paved streets. Other than a few trees, there is relatively little vegetation. The Dapperbuurt and Frederik Hendrikbuurt were built at the end of the 19th century, which is reflected in a similar architectural style. The Van der Pekbuurt, Marathonbuurt and Diamantbuurt were built between 1920 and 1930. The Marathonbuurt and Diamantbuurt have very similar characteristics and were built in the Amsterdam School architecture style. In contrast to other neighbourhoods, the Van der Pekbuurt can be classified as a garden city, that mainly contains single-family dwellings, often with a large amount of surrounding greenery.

The Van der Pekbuurt is currently under construction for renovation work, which may imply a rise in the energy labels of most buildings. The public space in the Frederik Hendrikbuurt is currently being completely redesigned, adding large patches of green space which are expected to reduce the UHI (Gemeente Amsterdam West, 2014). This makes buildings in these neighbourhoods less applicable for this research. As the buildings in the Dapperbuurt contain larger windows that minimize the possible surface area of facade vegetation, the houses in this area have not been further investigated either.

Dwellings in the Marathonbuurt and Diamantbuurt were both considered suitable. It is decided to focus for this research on the dwellings in the Diamantbuurt due to the availability of data on this neighbourhood. As several buildings from the Saffierstraat fell within the 95 percent confidence interval, a section of this street (surrounding number 13) was chosen as the study area.

4. 3. Study area specifics and model input

The Diamantbuurt, consisting of streets with diamond-related names, is a neighbourhood within Amsterdam Zuid. It was built in the 1920s in the Amsterdam School style of architecture, designed by J. C. van Epen. Almost the entire district was renovated in 1977, adding central heating and showers in all apartments. In a later renovation in 2007, asbestos was removed. The current energy labels of the housing corporation dwellings in the Saffierstraat vary between E and F and the UHI effect shows for the entire street a difference of more than 2 degrees Celsius compared to rural areas. In this section parts that are incorporated in the ENVI model of the study area are described: the insulation of the buildings, the soil, weather data and the facade greening.

4. 3. 1. Insulation

Despite the renovation in 1977, signs of any extra insulation aren't present at any of the drawings or files (Building Archive Municipality of Amsterdam, 2020). To verify this a calculation was carried out based on the lambda value of the bricks, the thickness of the wall and building policy at the time of the renovation.

The lambda value of a material indicates its ability to transfer heat and is expressed in W/m.K. Together with the thickness of the layer in meters (s) it accounts for the thermal resistance of a material (R-value) in the following way:

$R = s / \lambda$

Where R is expressed in m2K/W.

The lambda value (heat conductivity of a material) of red brick stones varies between 0.59-0.85 (Kort, 2009). Based on the thickness of the brick wall of 0.22 m (derived from the drawing of the buildings) this results in an R-value of 0.22/0.59=0.41 m2 K/W. In the 1960s, just before the renovation, it was suggested that if central heating was present in a building, the insulation value of the building should be 'sufficient' (Ministerie van Volkshuisvesting en Ruimtelijke Ordening, 1969). Since the mandatory R-value for that period was 0.43 and central heating was added in the renovation, it is assumed that no extra insulation was added to the walls.

This physical aspect of the buildings in the Saffierstraat was incorporated in the simulation model using the default Brick (burned) material was used for walls. In ENVI-met every wall is made up out of 3 different layers, with a default thickness of 0.30 meter. A wall thickness of 0.22 meters was derived from the building plans, which was subsequently used in this study. Consequently, this translates to a wall of 3 parts of 0.07333 meters (adding up to 0.22) in

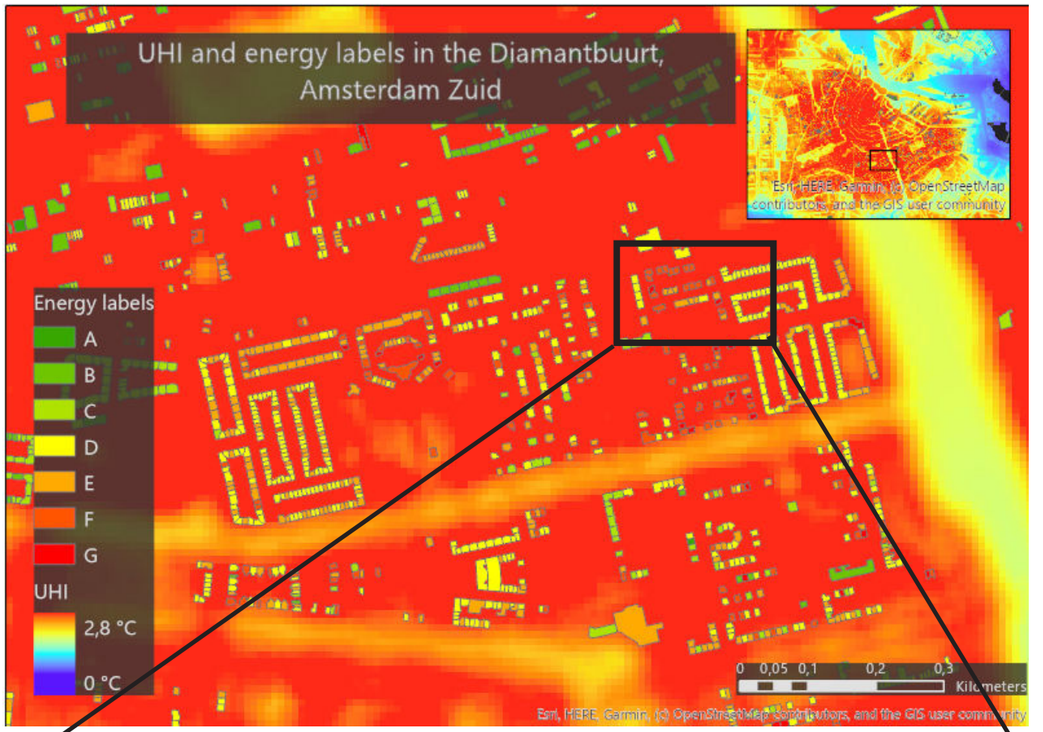

Figure 15 UHI and energy labels in the Diamantbuurt

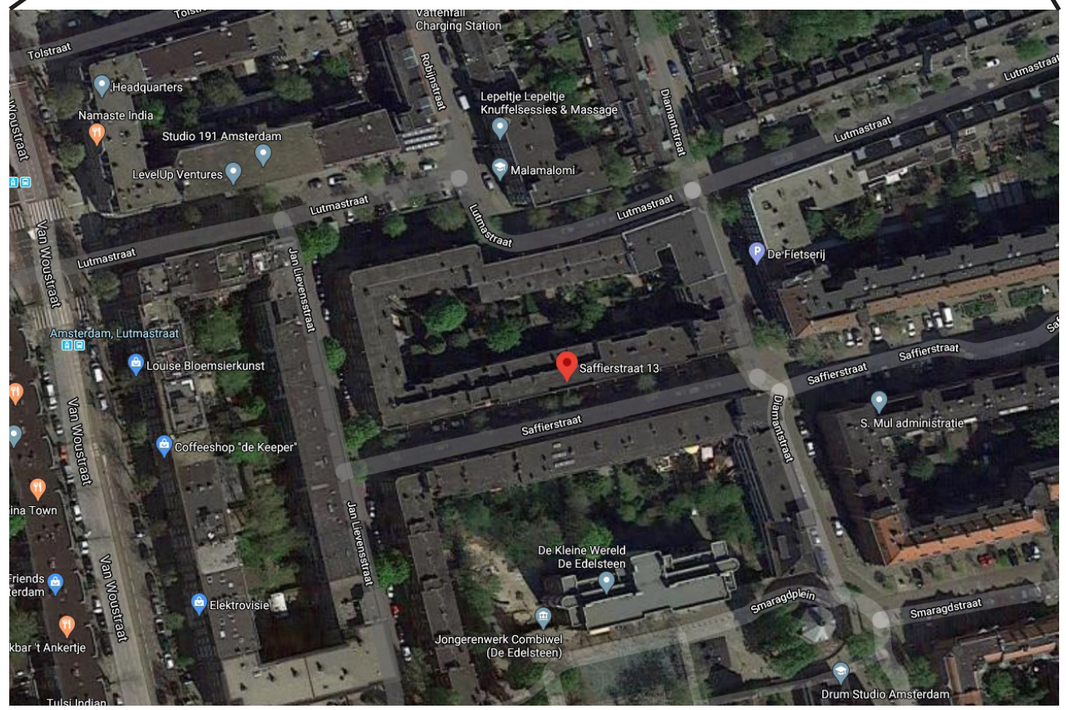

Figure 16 Sateillite image of the Diamantbuurt with the Saffierstraat identified with the red point. Derived from https://maps.google.com/

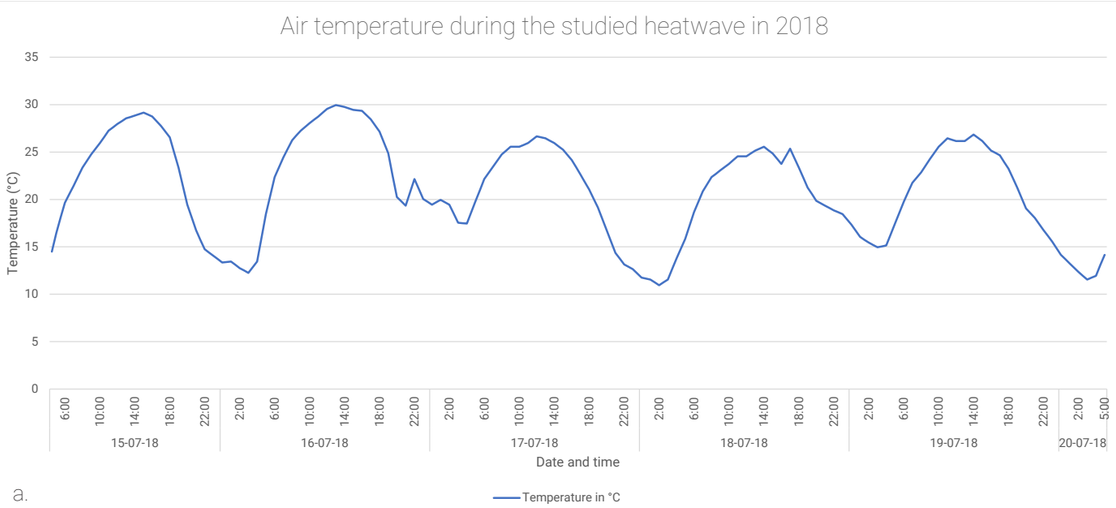

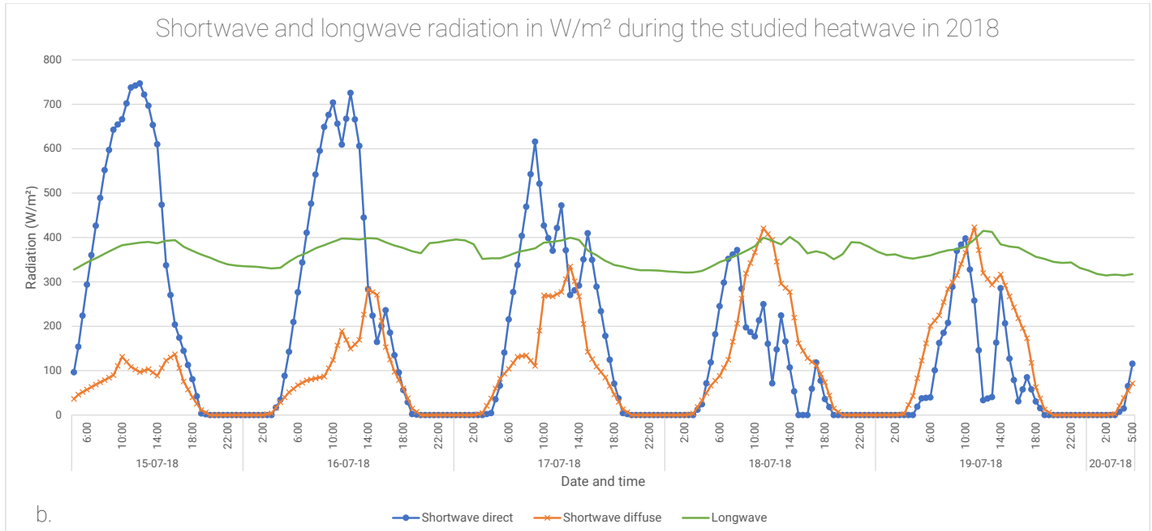

Figure 17 Selected heatwave climate data from Veenkampen weather station from July 15th to July 20th 2018. a. shows the measured air temperatures and b. the direct shortwave radiation, diffuse shortwave radiation and longwave radation measured at the time

ENVI-met. All other default parameters of the building materials were kept constant.

4. 3. 2. Soil and weather data

Amsterdam is built on a peaty soil. However, the top layer of the soil is an anthropogenic layer, which consists of a combination of bricks, sand and other materials. Since the ENVI-met software requires sandy loam as a basis for simple vegetation such as grass, this soil type was used for greened areas in model simulations.

Meteorological data of 2018 was used from the weather station in Veenkampen, near Wageningen. Data from this station contains detailed information on radiation components, which is an advantage when using it to drive ENVI-met. At Veenkampen shortwave direct

Figure 18 A H. helix and Parthenocissus at the Pieter Lastmankade in Amsterdam Zuid. Picture by Maarten Wesselink, derived from https://nmtzuid.nl/2017/12/01/fraaiste-groene-gevels/

radiation, shortwave diffuse radiation and longwave radiation are observed, which avoids the need to use parameterisations to assess these quantities for use in ENVI-met. Data was selected from a period from 15 to 27 July in 2018 in which several heatwaves took place. The period between the 15th and 20th of July was selected for this research. Figure 17 shows the air temperature, direct shortwave radiation, diffuse shortwave radiation and longwave radiation that were used in the present study. Hourly Veenkampen data was interpolated to obtain half-hourly data as required by ENVI-met. Pre-processing of dates, time and interpolations were done in Excel.

4. 3. 3. Green facades

H. helix and *Stachys byzantina* were associated with the greatest overall cooling in an experimental setup by Cameron et al. (2014). Both species form a dense foliar canopy in front of a wall. *H. helix* was used in this research as green facade, since it is commonly used in gardens in Western-European countries and has proved to decrease the facade temperature by shading. It is known as a self-climber, which can reach heights of 20 meters or more Figure 18. Flowers grow in September, which attracts various species of bees. Its fruits attract birds after the winter period. The species performs best in sunny to semi-shaded positions.

In the ENVI-met model a plant thickness of 0.30 meter was used, with a LAI of 1.50 m2/m2 and a leaf angle distribution of 0.5. A summary of the building, vegetation and pavement specifics used in the ENVI-met simulations are given in Table 4.

Model section	Material		Value	Unit
Researched building	Brick walls	Thickness	0.22	m
		Absorption	0.6	
		Reflection	0.4	
		Emissivity	0.9	
		Specific Heat	650	
		Thermal conductivity	0.44	W/(m*K)
		Density	1500	
Windows	Clear float glass	Thickness	0.03	m
		Thermal conductivity	1.05	W/(m*K)
Other buildings	Default wall: moderate insulation			
Green facade	Hedera helix	Plant thickness	0.3	
		Leaf area index (LAI)	1.50	m2/m2
		Leaf angle distribution	0.5	
Pavement				
Trees	Spherical, medium trunk, sparse, small		5	m (height)
Soil	Default unsealed soil (Sandy loam)			
Grass	Grass, 25 cm average, dense			

Table 4 Model parameters

5. ASSESSING INDOOR AND OUTDOOR TEMPERATURES USING A MODELLING APPROACH IN ENVI-MET

5. 1. Pre-analysis: Justification of grid size and study area size in ENVI-met

In ENVI-met both grid size and study area size can affect the outcomes of simulations. Firstly, depending on the grid size, buildings and trees can vary in the level of detail they contain, where smaller grid sizes are more precise than larger grid sizes. The calculations over the cells are subsequently altered, affecting the outcome of the simulation. To rightfully test the impact of green facades both inside and outside, both aspects should contain enough level of detail. Secondly, the size of the study area can influence the results around green facades. Factors that occur at street or neighbourhood level, such as wind tunnels or shadows from the opposite side of the road, can influence the PET and inside air temperature as well. Considering the optimization trade-off of producing a reliable result within the shortest computation time possible, a computational sensitivity check was performed to determine the sizes of the grids and the study area.

5. 1. 1. Grid size sensitivity check

Three 24-hour simulations were performed with different grid sizes: small (1x1x1m), medium (2x2x2m) and large (3x3x3m) (Figure 19). The model outcomes were compared for air temperature, PET and inside air temperature. The outside temperatures were determined 1.5 meters above the ground, with a distance of 1 to 1.5 meters from the wall, depending on the grid size. To limit local deviations, the average was calculated over an area of 2x6 or 3x6 meters (depending on the possibilities of the grid) for 24 hours. As more accurate results can be obtained in the smaller grid cell, it is assumed that this is most representative of the urban microclimate. The other two grid sizes are therefore compared with the smaller model. Differences caused by the grid size of more than 1 °C in the average temperature over 24 hours were considered undesirable.

For both potential air temperature and PET the differences between the small, medium and large model remained below 1°C over 24 hours (Figure 20). Hourly comparisons of potential air temperatures showed a peak difference of max 2°C in the morning for the medium and large model compared to the small model, but remained below 0.5 °C in the rest of the simulated period. For PET these differences were larger, but only within the time frame of 10 am to 1 pm; after that, these differences remain below 1 °C. The average temperature differences in indoor temperature between the small and medium grid sizes over 24 hours were marginal (<0.1°C), while the inside air temperature reached peak differences to the

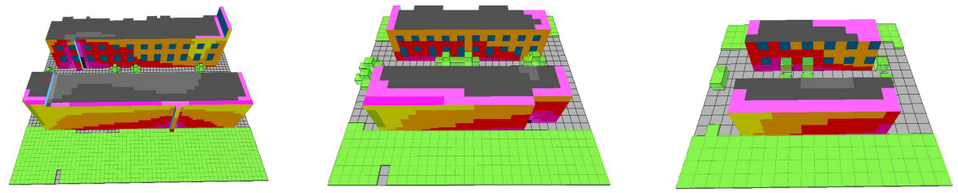

a. b. c.

Figure 19 The different grid sizes with in a. small (1x1x1m), b. medium (2x2x2m) and c. large (3x3x3m).

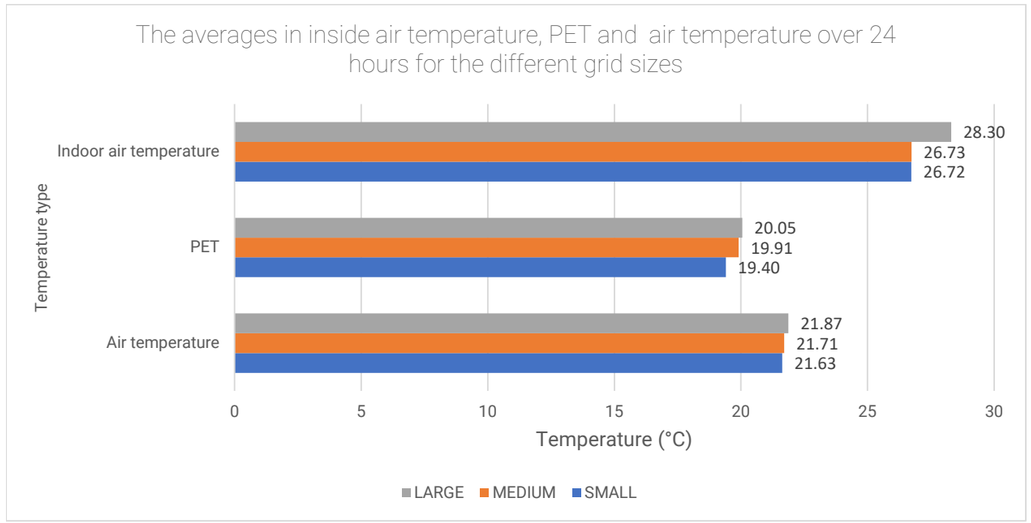

Figure 20 Average indoor and outdoor temperatures measured in different grid sizes

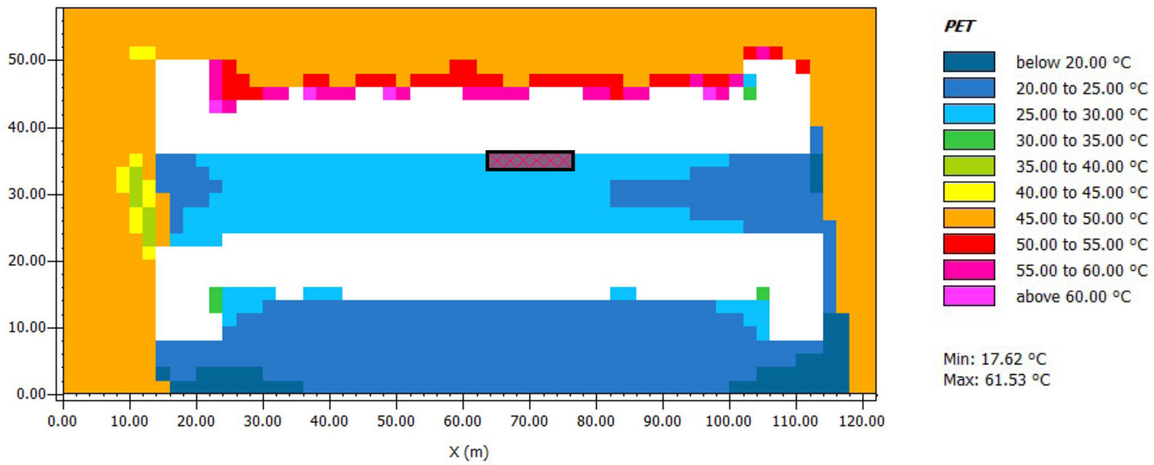

Figure 21 Selected grid cells used for evaluating air temperature and PET. The red box indicates the studied grid cells (2x2m per cross). Pet values are an example for clarification

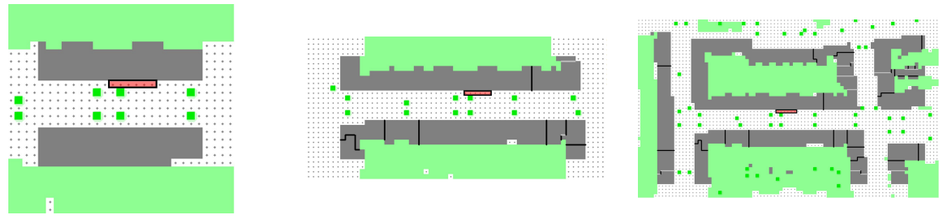

a. b. c.

Figure 22 The different study area sizes in Spaces with in a. small, b. medium and c. large. Red boxes indicate the studied grid cells

other models of 4°C between 6 am and 11 at night. Since the medium and small model show deviations below the threshold value of 1°C while the large grid size exceeds this, a 2x2x2 grid is used in this study.

5. 1. 2. Study area size

To test possible effects of the study area size, three different study areas were compared for the 2x2x2 grid: a small area, with 3 houses on one side of the street and 3 on the opposite side, a medium area with the entire street and a large area, with the entire housing block (Figure 22).

Air temperature and PET were determined based on the six selected cells in Figure 21. A small deviation from the centre of the block was made to limit the effect of the trees in the street on the PET out-comes. All results were obtained at a height of 1.4 m (third model level). Over the six cells the mean was calculated and used for the analysis of the results. The inside building temperature was evaluated in the middle of the six studied cells at 2 meter above the ground.

All three simulations were performed for 24 hours and measured on potential air temperature, PET and inside air temperature. Here it is assumed that the largest model is the most reliable. Therefore, the values of the other study area sizes are compared to this model. Again a 1 °C threshold was used.

The largest study area size resulted in higher potential air temperature and PET over 24 hours than for the other study areas, but remained within a 1°C difference (Figure 23). A decrease in study area size resulted in a decrease in PET: 27.63°C (large), 27.46°C (medium) and 26.94°C (small). The indoor temperature increases when comparing the small and medium models (27.16 for small, 27.37 for medium) but decreases in the large model (26.66). Simulation time increased from less than 2 hours for the small model, to 4 hours for the medium model and more than 13 hours for the large model. As all results fall within the threshold difference of 1 degree Celsius, but the simulation time increases drastically, the medium study area is used considering the optimization problem.

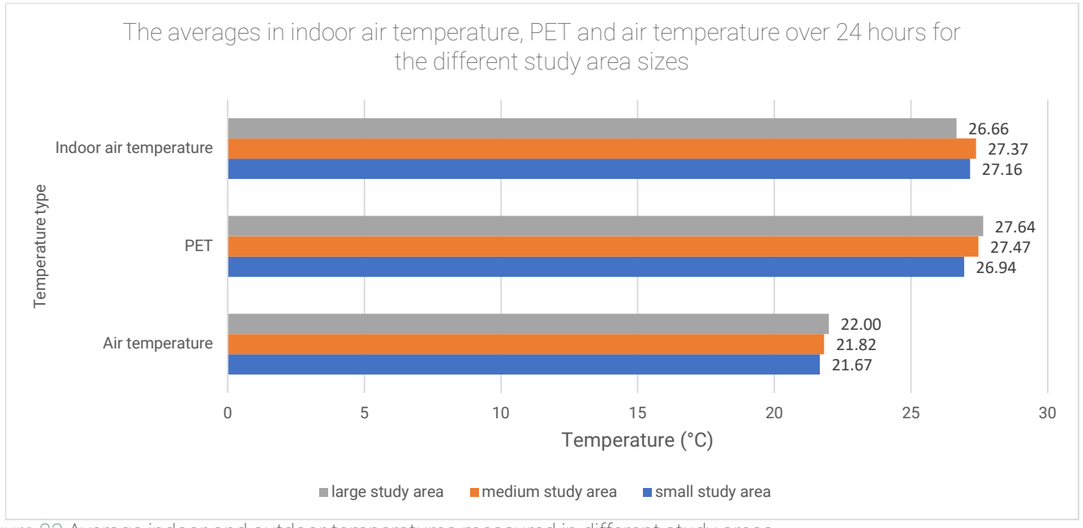

Figure 23 Average indoor and outdoor temperatures measured in different study areas.

5. 1. 3. Model setup

Table 5 provides an overview of the model characteristics based on the grid size and study area sensitivity check described in the previous sections. Other characteristics are given as well. All simulations were performed for 5 days to incorporate the slow heat accumulation in buildings. The tallest building in the model domain has a height of 19 m. ENVI-met requires a higher boundary to perform its calculations reliably, hence the height of the upper boundary of the domain was set at 42 meters. All input variables are shown in Table 5.

Since building orientation can highly affect the microclimate, indoor temperature and the effect of green facades, the study area was tested for facade openings facing north, east, south and west, with and without green facades. The simulation is perceived as north-oriented if the front side of the Saffierstraat 13 is facing that direction. The standard orientation of the Saffierstraat is -14 degrees out of grid north. Figure 24 shows the different orientations simulated. In the simulations with greened facades the greening covered the studied facade of the entire building block, apart from the windows. Table 6 provides an overview of all simulations. PET values were calculated in Biomet, using the standard body and clothing parameters provided by the program (Table 7). To assess indoor temperatures the inner and outer node of the seven prognostic calculation nodes of walls were used as established by ENVI-met. For the outside node, the meteorological parameters and thermal state of the buildings are considered, while the thermal state of the inner node is calculated from the physical properties assigned to the wall. Throughout the rest of this research these will be referred to as inside and outside node.

Model input	Specifics
Simulation model size (m)	122 x 58 x 42
Model area (number of grids)	61 x 29 x 21
Size of grid cell (m)	2 x 2 x 2
Geographic location (latitude, longitude)	52.35, 4.90
Nesting grids	0
Method of vertical grid generation	Equidistant
Reference time zone	Central European Standard Time
Main model parameters	
Simulation date	15 July 2018
Start and duration of simulation	05:00, 120h (5 days)

Table 5 Input data of the studiy area in ENVI-met

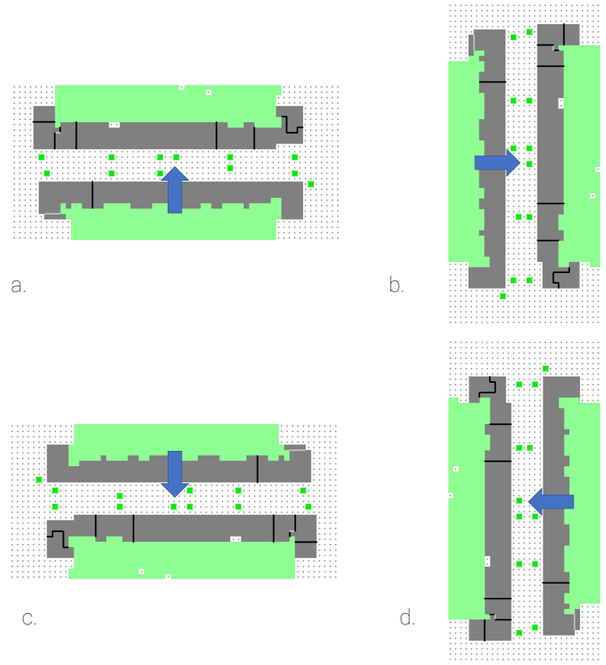

Figure 24 visualisation of the different building orientations with in a. north -oriented, in b. east-oriented, in c. south-oriented and in d. west-oriented studied buildings

Model name	Orientation	Degrees out of grid north	Period	Green facade
Saffierstraat north	north-south	166	05:00, 15/07/2018 – 05:00, 20/07/2018	No
Saffierstraat east	east-west	256	05:00, 15/07/2018 – 05:00, 20/07/2018	No
Saffierstraat south	south-north	346	05:00, 15/07/2018 – 05:00, 20/07/2018	No
Saffierstraat west	west-east	76	05:00, 15/07/2018 – 05:00, 20/07/2018	No
Saffierstraat north green	north-south	166	05:00, 15/07/2018 – 05:00, 20/07/2018	Yes
Saffierstraat east green	east-west	256	05:00, 15/07/2018 – 05:00, 20/07/2018	Yes
Saffierstraat south green	south-north	346	05:00, 15/07/2018 – 05:00, 20/07/2018	Yes
Saffierstraat west green	west-east	76	05:00, 15/07/2018 – 05:00, 20/07/2018	yes

Table 6 All simulations performed in ENVI-met

Age	Gender	Weight (kg)	Height (m)	Static Clothing Insulation (clo)	Metabolic rate
35	Male	75	1.75	0.60	164.49

Table 7 Default variables for PET calculations in Biomet

5. 2. Modelling results: evaluating the effect of green facades and building orientation on temperatures

5. 2. 1. Air temperature

Effect of green facade

The air temperature in front of the buildings with and without a green facade differed most between 12 and 3 pm (see Figure 26) These differences amounted to a maximum of 0.35 °C for the northern orientation, but were more pronounced for the south (0.65 °C), east (0.48 °C) and west oriented study area (0.55 °C). Figure 26 shows the spatial air temperature patterns for the southern orientation.

The surface temperatures of the outside node of the wall showed a decrease of 3 to 5 °C when a green facade was present compared to the bare wall at 14 o'clock on the first simulation day for the southern orientation (Figure 25). These differences were less pronounced at the same moment in the following days or at different moments in time.

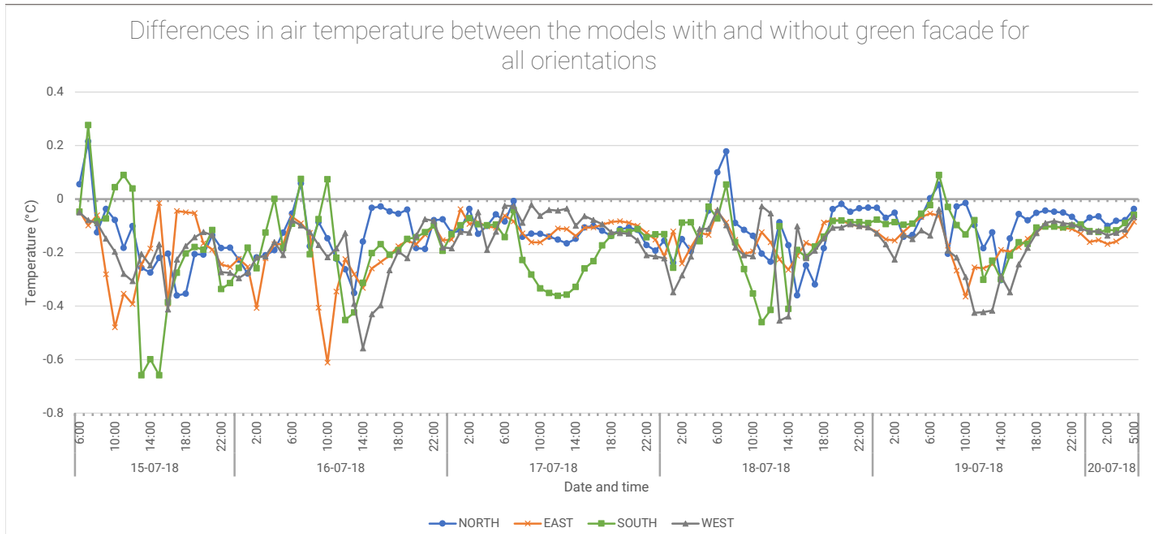

Figure 26 differences in air temperature for the different orientations

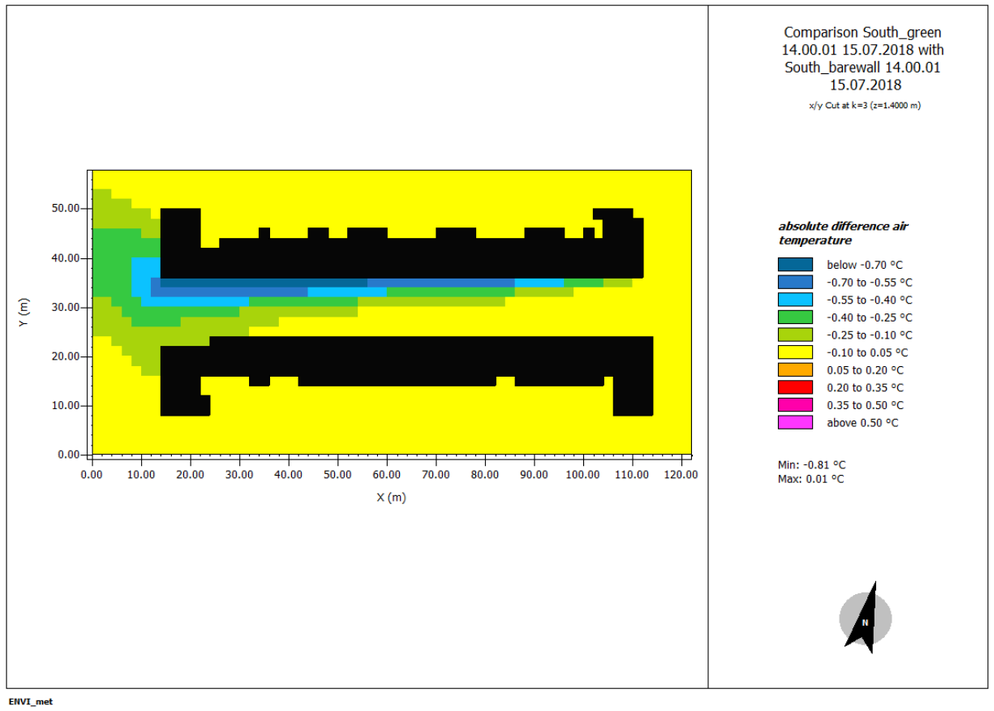

Figure 25 Differences in potential air temperature at 2 pm for southern orientation with and without green facades

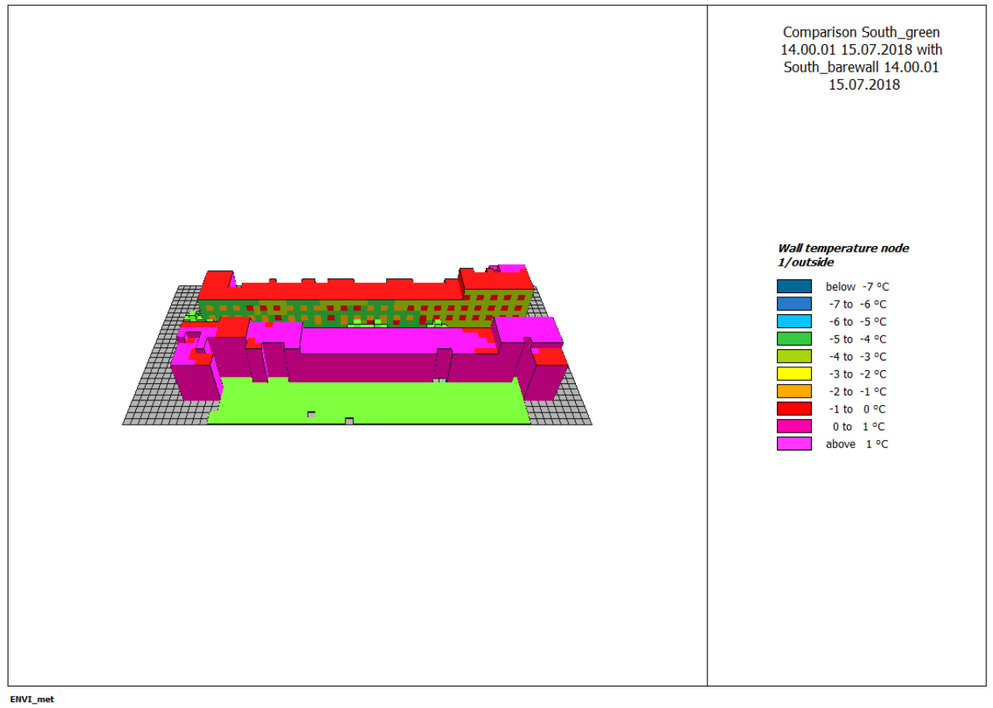

Figure 27 Differences in surface temperature at the outside node of the wall at 2 pm for southern orientation with and without green facades

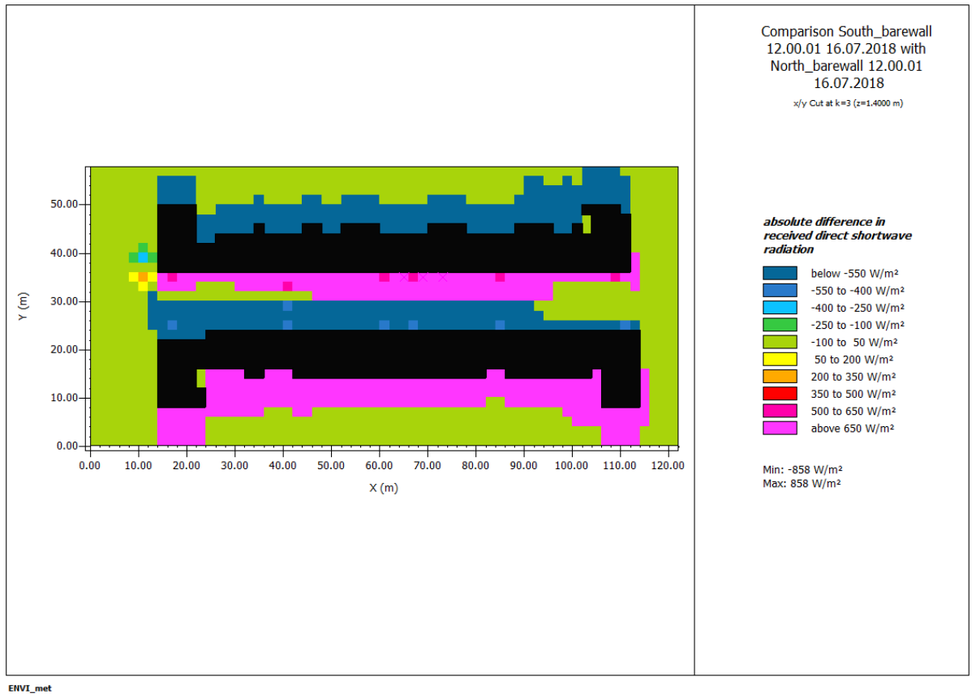

Figure 28 Absolute difference in shortwave radiation at 12 pm for the southern (reference) and northern orientation

Effect of orientation

All orientations reached their maximum air temperatures between 12 and 1 pm on the second simulation day, resulting in air temperatures of 29.8 °C for the northern orientation, 30.8 °C for the east, 31.8 °C for the south and 30.9 °C for the west oriented model simulation. The maximum temperatures concomitantly take place with the largest differences between orientations, amounting to 2.36 °C between the cooler northern orientation and hottest southern orientation. Around noon the direct shortwave radiation from the sun differs the most for these orientations: the southern orientation receives between 750 and 900 W/m², while the values remain below 150 W/m² for the northern orientation (Figure 28). The differences in reflected shortwave radiation at that time remained below 1 W/m². Wall temperatures at 12 pm differed widely among orientations: the temperature at 12 pm was more than 12 °C lower in the east orientation compared to the south orientation. Since the sun rises in the east and sets in the west, the southern orientation receives the longest duration of direct sun relative to other orientations. The shortwave radiation received at the measured cells is visualised in Figure 29.

In the first two days of the simulation the highest air temperatures are reached for all models (> 30 °C) and these decrease in the following three days. This pattern corresponds with the input temperature and shortwave radiation values as described in Figure 17.

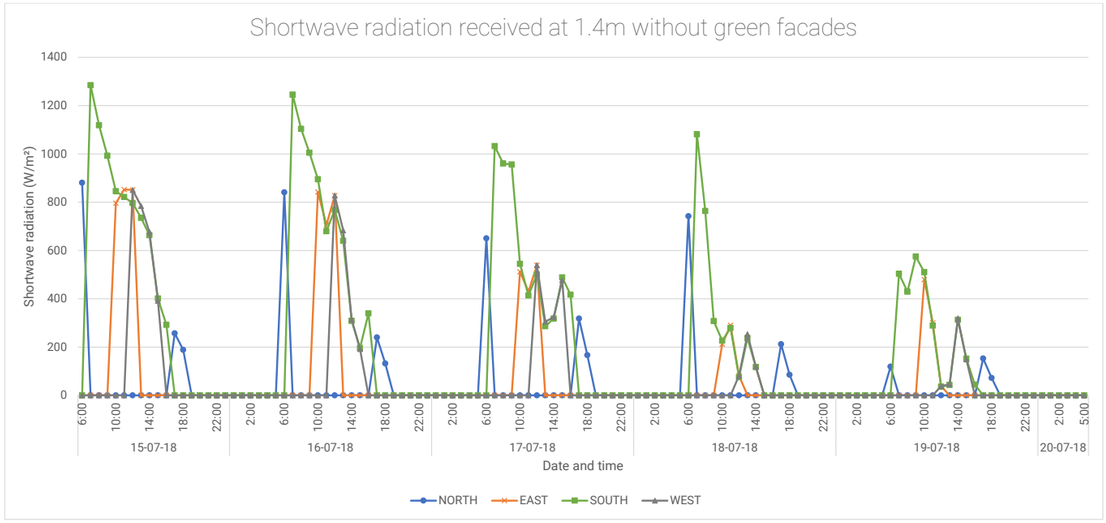

Figure 29 The amount of shortwave radiation measured in front of the wall at 1.4 meter above the ground for all orientations

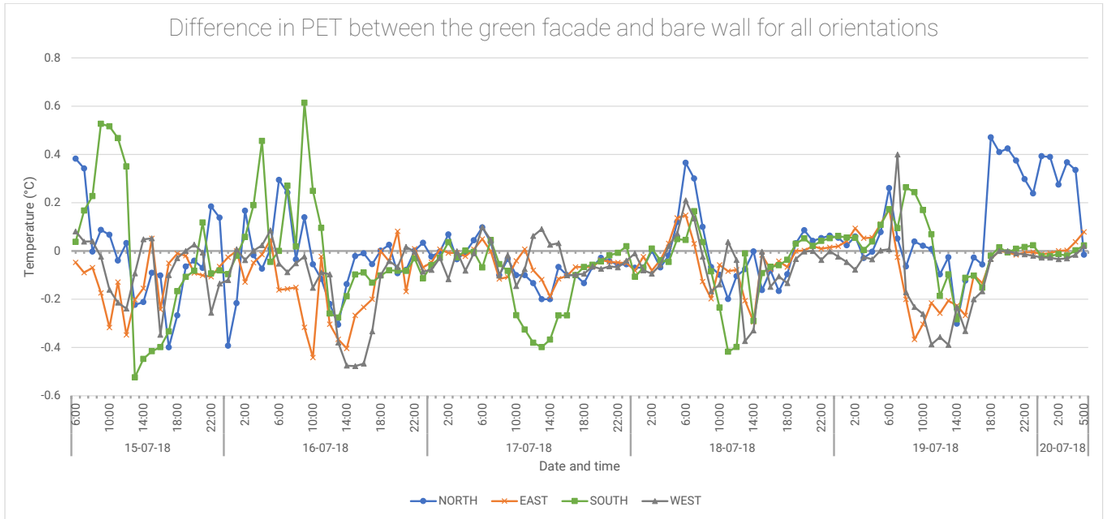

Figure 30 Difference in PET per orientation with and without green facade

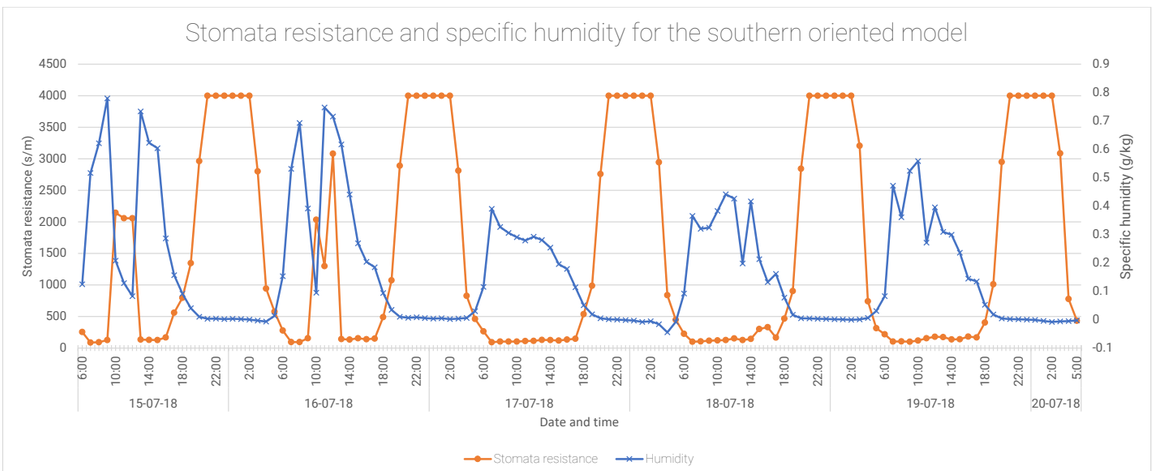

Figure 31 Stomatal resistance and specific humidity for the southern oriented simulation model

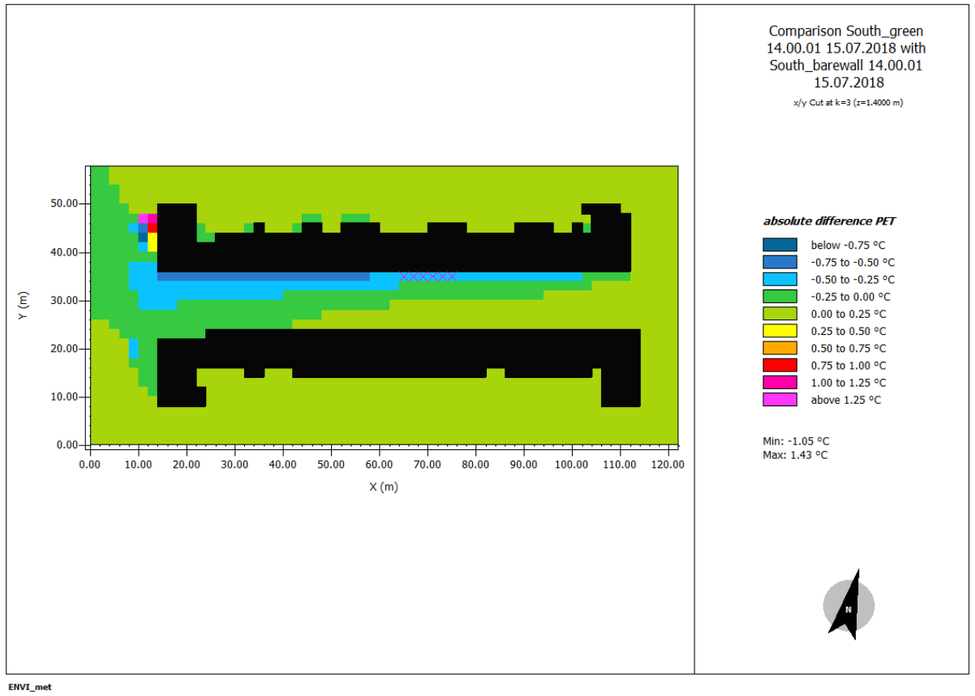

Figure 32 Absolute difference in PET at 2 pm between the bare wall and greened facade for the southern orientation on the first simulation day.

5. 2. 2. Physiological Equivalent Temperature

Effect of green facade

The differences between the buildings with bare facades and buildings with green facades remained in all cases below 0.7 °C. These differences were both positive as negative, indicating that a green facade can both increase and decrease PET values (Figure 30). No clear time pattern can be discerned when the PET of the green facade differs from the buildings without the green facade as this was different in all model comparisons. As the differences in PET caused by green facades only amounted to values below 1 °C, the effect on thermal perception is marginal as this uses classes of 4 °C (Andreas Matzarakis & Mayer, 1996). On the first simulation day the southern model firstly showed higher PET values (0.5 °C) for the model with the green facade before noon, while this changed to lower PET (-0.5 °C) shortly after. These differences were most apparent directly in front of the (greened) wall (Figure 32).

Of the four major meteorological parameters that influence PET, the largest deviations occurred for the mean radiant temperature on the first simulation day for the southern oriented facade: The greened wall showed an increase of 0.5 °C in T_{mrt} before 12 pm, which relates to a higher reflection rate of shortwave radiation of the greened facade (difference of 83 W/m^2). This corresponds to a peak in specific humidity (q = 0.8 g/kg). Differences in windspeed and air temperature are neglectable (v=0.01 m/s, T_a= 0.2 °C). Generally, PET follows the pattern of T_{mrt}.

The highest positive peak in PET on the second simulation day from the southern model corresponds to a higher mean radiant temperature in front of the green facade compared

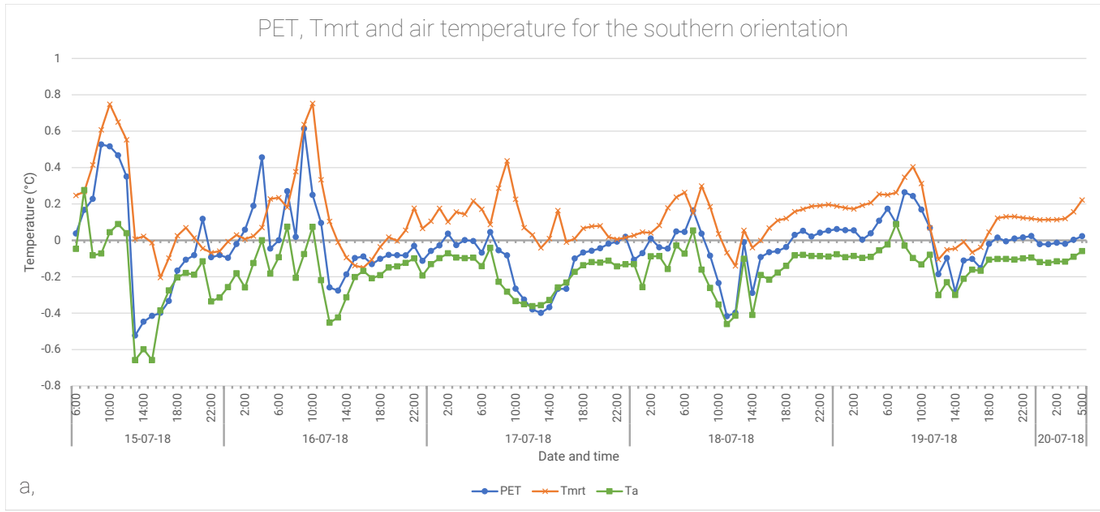

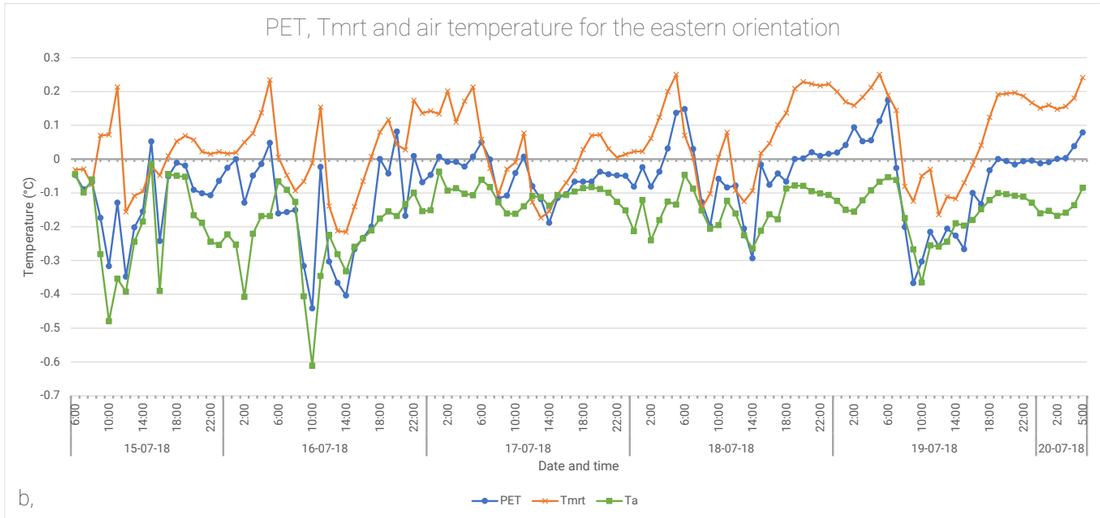

Figure 33 PET, T_{mrt} shortwave radiation over 120 hours with in a. the southern orientation and in b. the eastern orientation

to the bare wall. The larger amount of water vapor concentration corresponds to higher evapotranspiration rates by greened facades. Figure 31 shows the stomatal resistance and specific humidity for the southern oriented model. According to the results of the calculations, the green facades increase the humidity, but not enough to prevent the stomata from closing when the air is too dry.

For other orientations similar diurnal patterns occur, where PET follows T_{mrt}'s pattern but is on average 0.2 degrees cooler than the mean radiant temperature. Air temperatures are in general slightly cooler than PET. Figure 33 shows the PET, T_{mrt} and air temperatures for the southern and eastern oriented study areas.

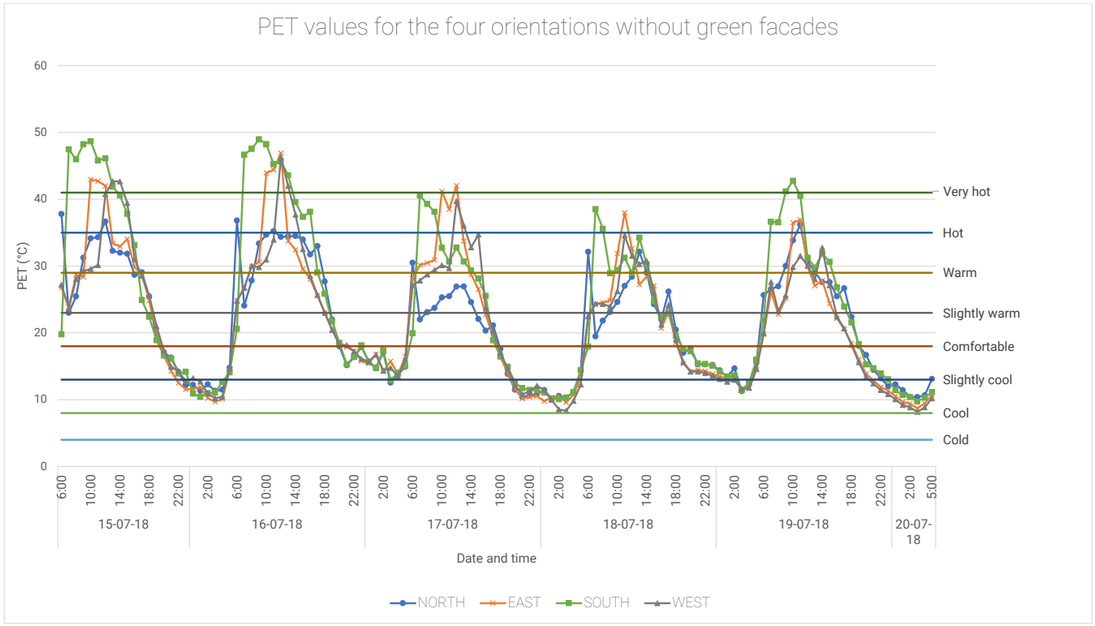

Figure 34 PET values for the four orientations without green facades

Effect of orientation

Orientation appeared to have a significant effect on PET, accounting for different maxima in PET and moments at which the maxima were reached. The maximum PET for the northern orientation was 38.1 °C, while the eastern, western and southern orientations exceeded 45 °C. For the southern orientation the PET values exceed the 41 °C threshold on three days with a maximum timespan of 10 consecutive hours (between 6 am and 4 pm on the 1st simulation day), corresponding to 'extreme heat stress' as described by Matzarakis and Mayer (1996) (Figure 34). The studied grid cells in the west and east orientated model simulations both experienced extreme heat stress three hours per day on the first two days, and strong and moderate heat stress at day time in the first three days. The northern oriented model reaches the lowest temperatures, corresponding to strong and moderate heat stress on the first days and slight heat stress on the last two days. At night all models show comparable patterns, equivalent to moderate and slight cold stress. Due to the larger amount of shortwave radiation and higher temperatures in the first two days of the simulation, the differences in PET between the orientations are more pronounced compared to the latter three days.

Of the four meteorological parameters influencing PET, the largest variation between orientation occurred for mean radiant temperature. Differences exceeded 20 °C between the north and south model. These values were reached in the parts of the model that were exposed to sun in one simulation, but were shaded in the other. Mean radiant temperature peaks in the studied grid cells of the east oriented model occurred at 11 am (64 °C), while the peak for the west orientation was reached at 2 pm (58.5 °C). Figure 35 shows the mean radiant temperatures of the west and east orientation at 11 am on the first simulation day. Locations shaded by trees showed a 3 to 6 °C decrease in mean radiant temperature. Peaks in shortwave radiation corresponded to peaks in mean radiant temperature obtained in the studied grid cells (Figure 36).

In terms of PET, air temperatures showed comparable diurnal variation patterns throughout the studied 120 hours for all orientations, apart from daily peaks in the afternoon (12 pm to 6 pm). The highest air temperatures in front of the facade occurred in the southern oriented

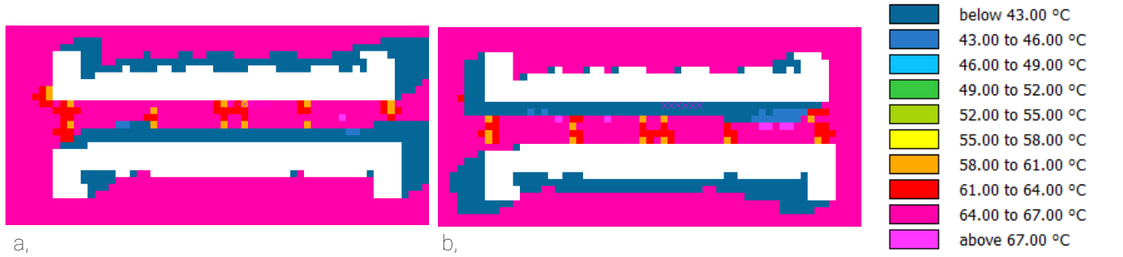

a, b,

Figure 35 Mean radiant temperature at 11 am on the first simulation day for a. the east oriented and b. the west oriented study area

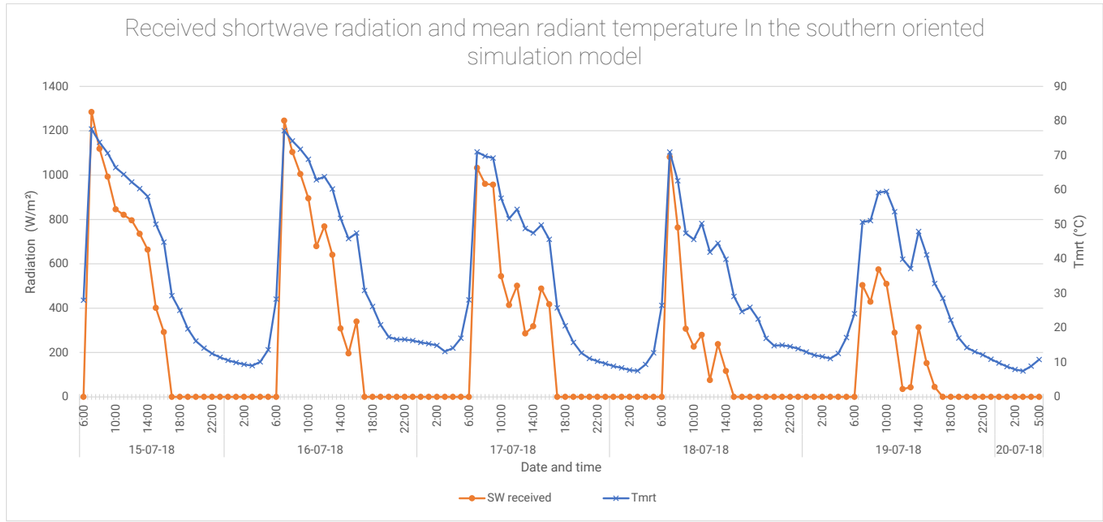

Figure 36 Received shortwave radiation and mean radiant temperature in the southern oriented simulation model

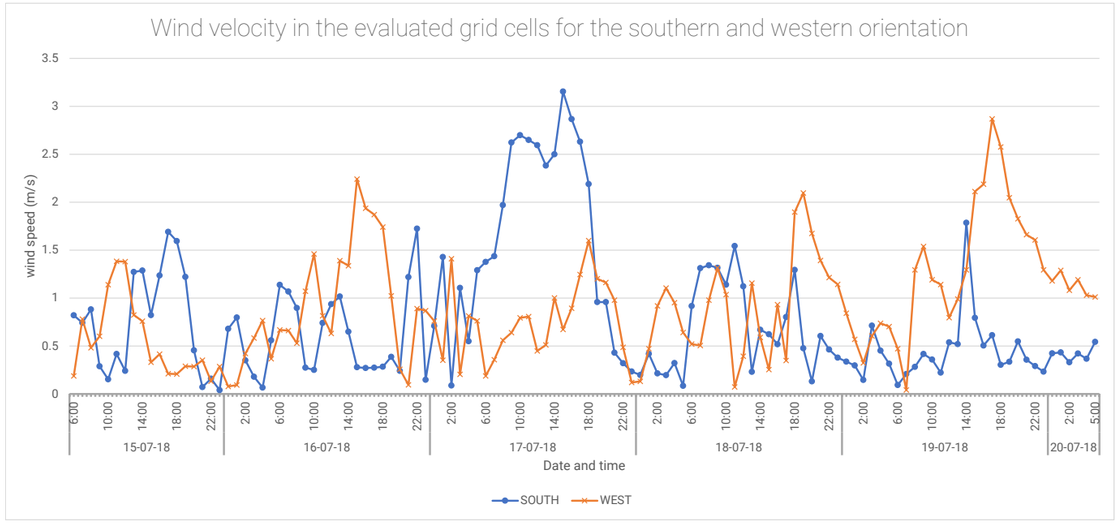

Figure 37 Differences in wind speed throughout the full simulation period for the southern and western oriented study area

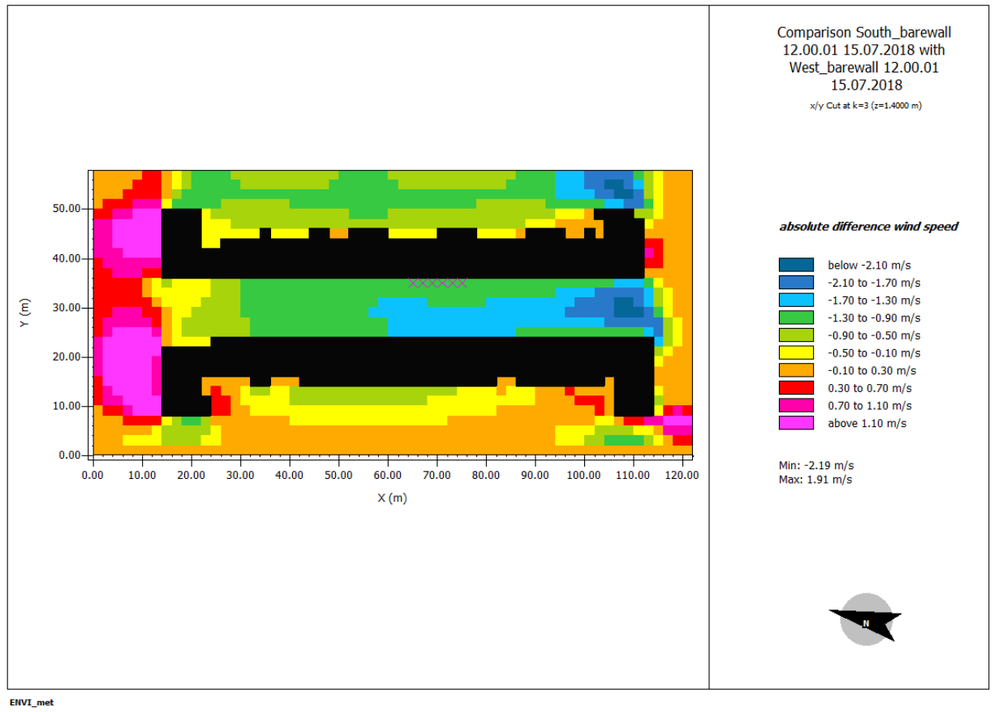

Figure 38 Difference in wind velocity at 12 pm between the southern and western orientation on the first simulation day

model, followed by the west, east and northern orientation. The input wind direction on the first simulation day was south-east, making the buildings in the south model blocking the wind, resulting in wind speeds of 0.33 m/s for the north and south oriented models around 12 pm. Higher wind speeds were obtained in the western and eastern orientations (1.42 m/s at the same day), as the wind could blow into the street for the west and east oriented buildings (Figure 38). After 12 pm, the wind increased slightly with 1 m/s for the southern model (Figure 37), which was accompanied by a decrease in PET (46.12 °C to 40.56 °C). Apart from small deviations, the north and south models show a similar pattern in terms of wind speed, as do the west and east model. The humidity values showed the same pattern in all models.

5. 2. 3. Indoor air temperature

The indoor air temperature at all orientations showed clear differences between the models with and without green facade, showing temperature decreases up to 3 °C for the southern orientation, 2.5 °C for the east and west and up to 1.8 °C for the northern orientation in the first two days. In the evening of the third simulation day these decreases shift to increases, resulting in higher indoor temperatures during the night and early morning in the presence of a green facade. During the afternoon and beginning of the evening the interior temperatures in dwellings with green facade were still lower than in buildings with bare walls.

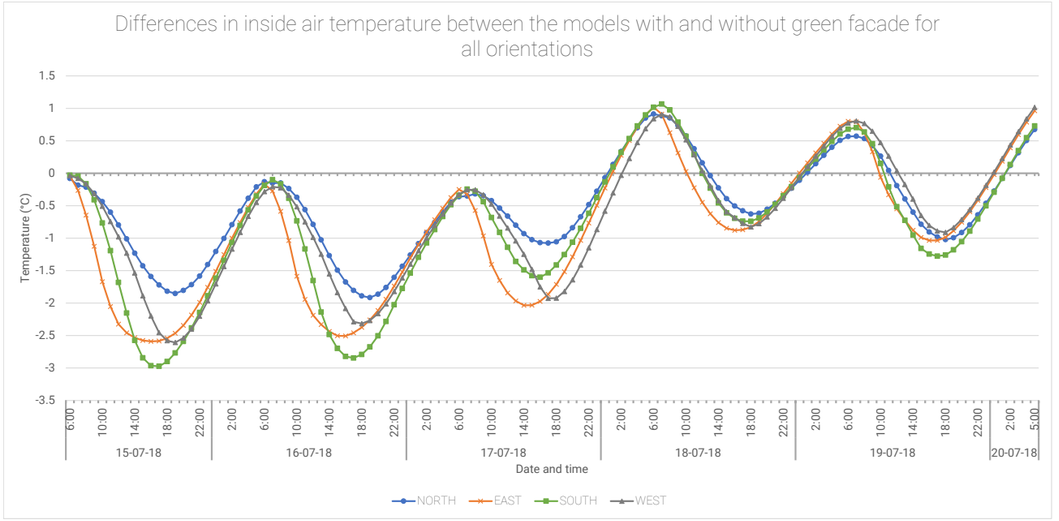

Figure 39 Differences in inside air temperatures between simulation models with and without green facade for all orientations

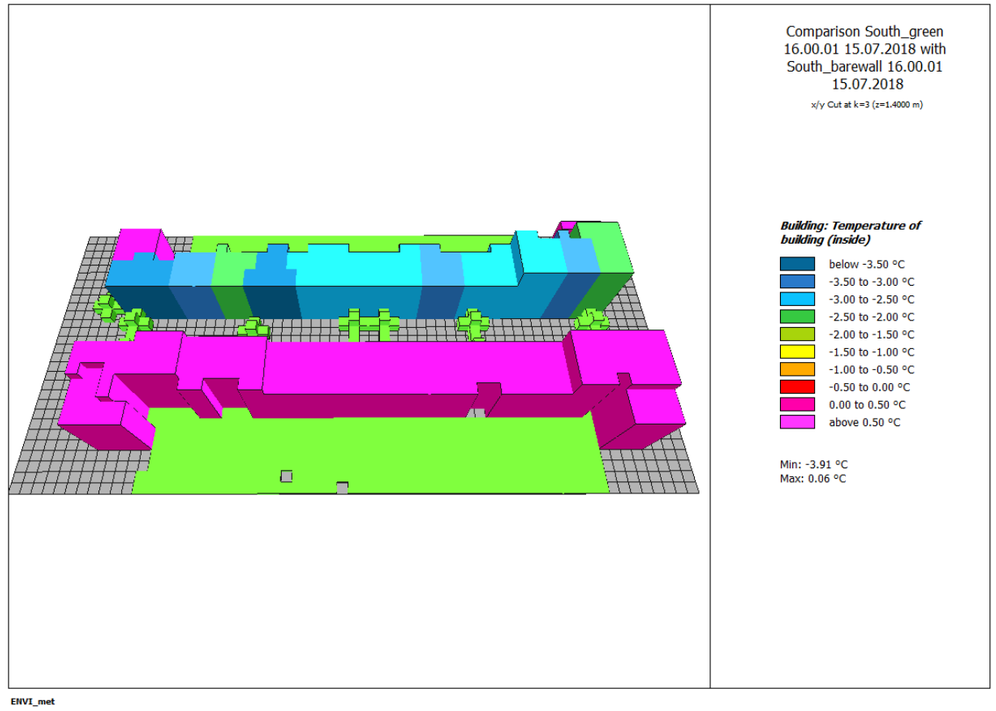

Figure 40 Difference in interior air temperatures between the bare wall and greened facade of the southern orientation at 4 pm on the first simulation day

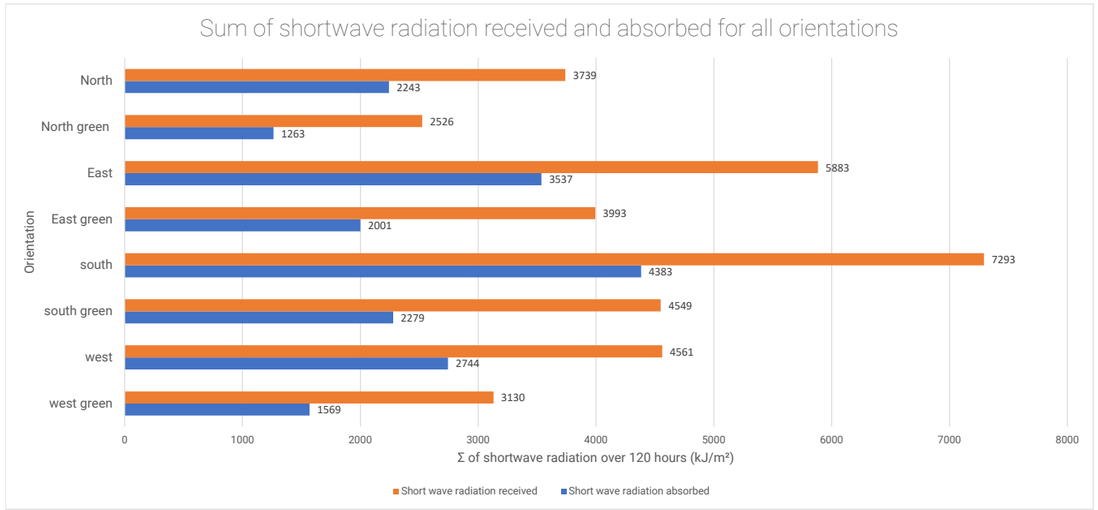

Figure 41 Sum of shortwave radiation received and absorbed for all orientations of a grid cell in front of the facade. Values are averages of the six studied grid cells at 1.4 m above the ground.

The walls with facade greening absorbed approximately 150 W/m² less shortwave radiation from the sun then the bare walls at 2 pm for the southern orientation, accounting for a 70% decrease at peak moments and a minimum decrease of 40%. The presence of a green facade reduced the received shortwave radiation by the wall over 5 days by more than 30 percent for all orientations and the absorbed shortwave radiation by more than 40 percent. While the outside node of the wall was still exposed to oscillating surface temperature differences, this stabilised for the inside node in the presence of facade vegetation. An example of these differences between the nodes for the east-oriented study area is given in Figure 44.

The largest differences in the presence of a green facade occur for the southern oriented study area (Figure 41). However, the highest indoor temperatures with a green facade still occur in the western and eastern oriented models. Since the southern oriented study model receives and absorbs the largest amount of shortwave radiation, the 40% decrease of shortwave radiation is the largest difference and therefore accounts for the biggest change in inside air temperature.

Effect of orientation

The largest differences in inside air temperature between orientations occurred between 6 am and 10 pm. The largest differences between orientations occurred within this time frame on the third day of the simulation, accounting for 7 °C difference: a temperature of 30.6 °C was reached in the northern model, compared to 37.7 °C for the western orientation. The highest daily temperatures occurred in the west-oriented model simulation, followed by the east and south-oriented buildings. The north-facing row of houses experienced the lowest temperatures. Peak daily temperatures were first reached by the east model, followed by the south, west and north model, respectively (Figure 42). Due to the inclination of the sun the east model receives a large amount of shortwave radiation in the morning, which enters the building via the window. The solar radiation hits the top of the building of the southern orientation and only reaches the windows to a small extent due to the solar angle. The weste-oriented buildings receive the largest amount of shortwave radiation in the afternoon and the beginning of the evening, and due to the low elevation of the sun, a large fraction is transmitted through the glass. Although this fraction is similar to the eastern oriented buildings, higher

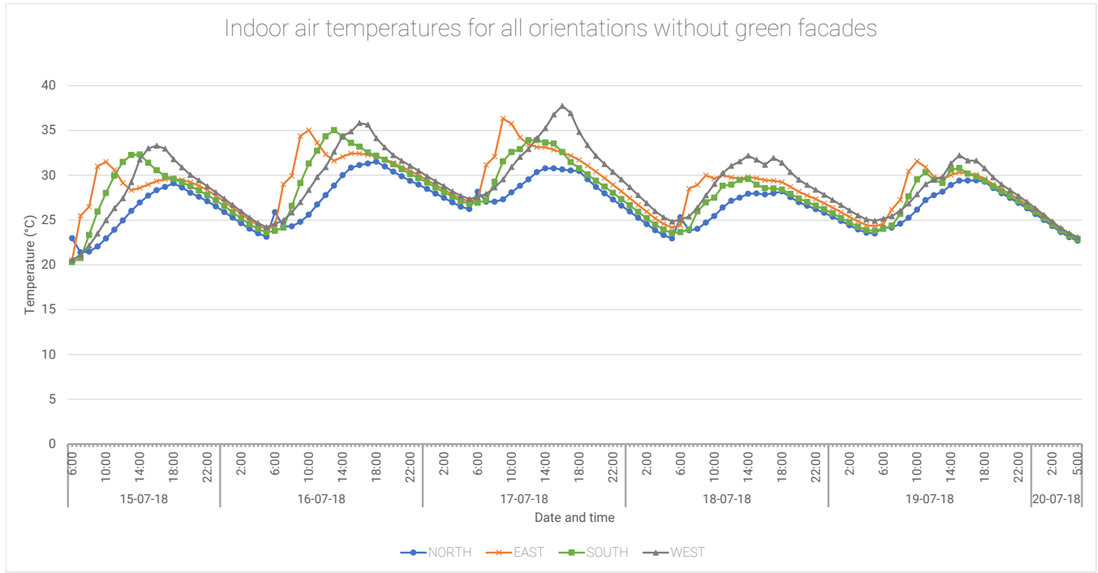

Figure 42 Indoor temperatures without green facades

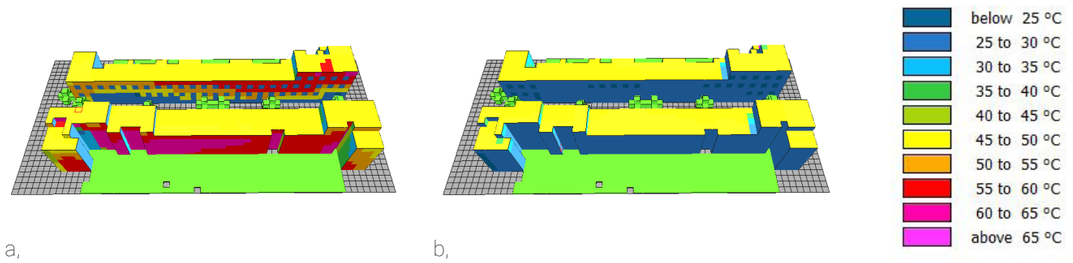

Figure 43 Wall temperature (outside node) at 9 am on the third simulation day for a. the east oriented and b. the west oriented study area

temperatures are reached in the west-oriented buildings since the air temperatures are lower in the eastern oriented buildings after overnight cooling. Figure 43 shows the difference in wall temperature at the outside node between the east and west oriented study area in the morning on the third simulation day.

The south oriented model received and absorbed the largest amount of shortwave radiation over the studied heatwave (adding up to 7293 kJ/m² and 4383 kJ/m² over 120 hours). The east oriented model received the largest peak amounts of shortwave radiation, accumulating to roughly 900 W/m² on the first 3 days. These numbers were significantly lower for the other orientation (south 600 W/m², west 400 W/m² and north 250 W/m²).

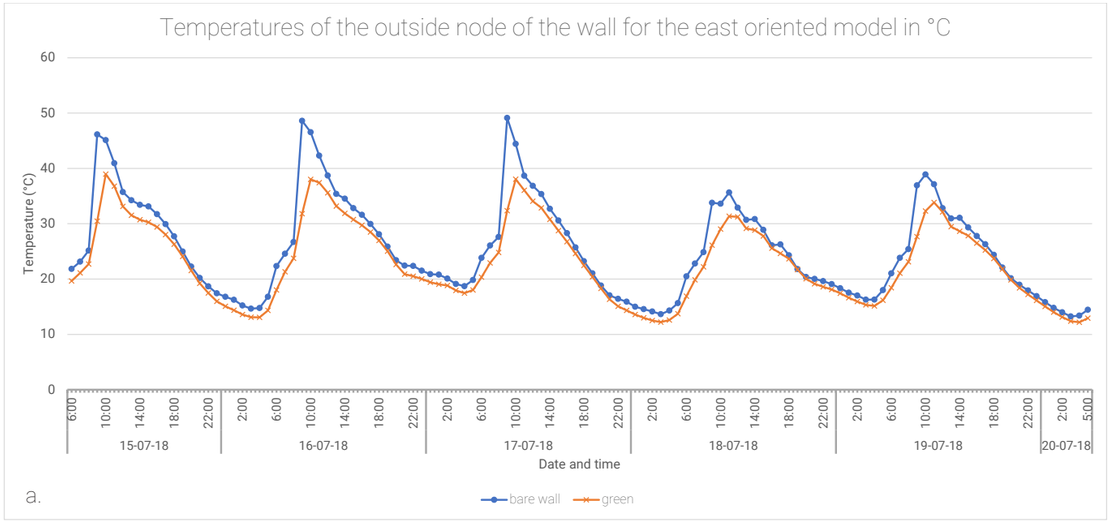

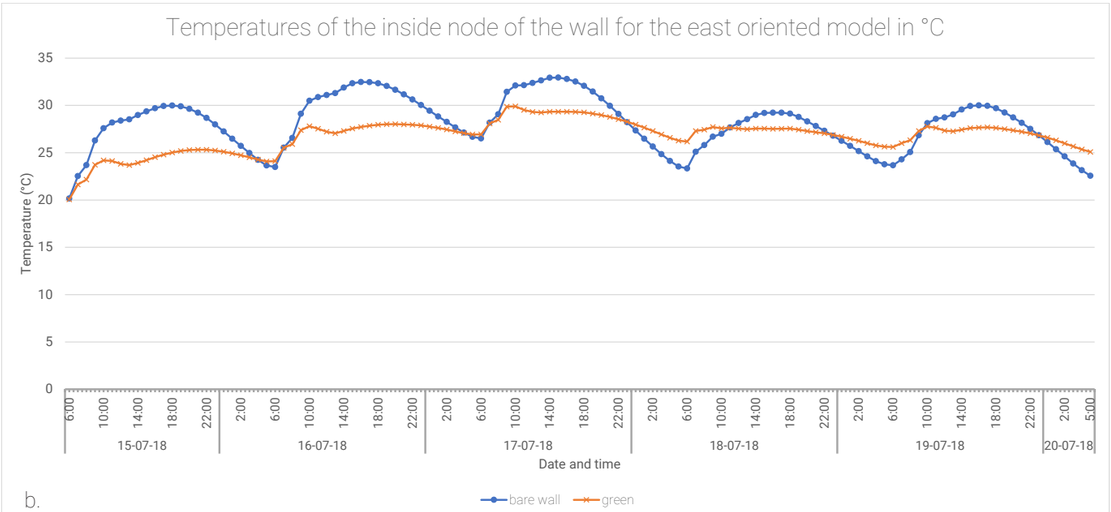

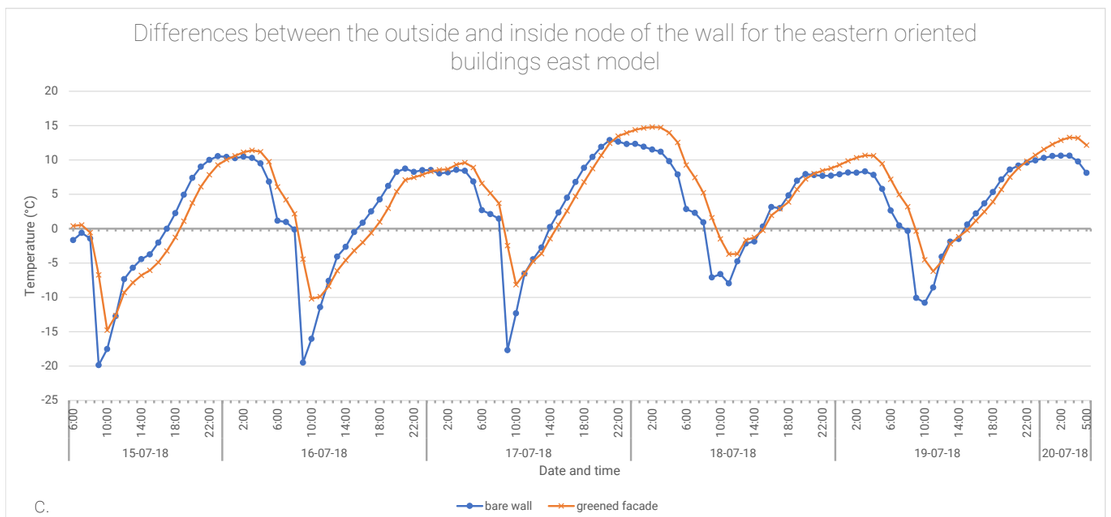

Figure 44 Surface temperature differences between the plain wall and greened facade with in a. outside node of the wall, in b. inside node of the wall and in c. the differences between the outside and inside node.

6. DISCUSSION

6. 1. Exposed dwellings in Amsterdam

The exposure and hot spot analysis identified several clusters of buildings of housing corporations within the Amsterdam municipality where indoor and outdoor temperatures could be problematic. These buildings and their local environment exhibited similarities in several respects: the streets were almost completely paved, there was little vegetation present and the buildings contained many large windows. Moreover, almost all identified buildings were built in building blocks.

Besides the other clusters, the study area ultimately used bears great resemblance to many other neighbourhoods in Amsterdam. Especially neighbourhoods that were developed between the end of the 19th century and the 1940s show comparable characteristics due to the similar streets, large windows and use of construction materials. Depending on the heat exposure and building and neighbourhood characteristics, the implementation of green facades in these places could be promising.

6. 2. Outdoor temperatures

Air temperature

The effect of green facades on air temperature in front of the wall amounted to a maximum decrease of 0.65 °C. These findings are in line with previous research, showing differences of 1.5 °C, 1°C, 0.25 °C and negligible changes in air temperature, respectively (Berry et al., 2013; Gross, 2012; Perez et al., 2011). Larger differences of 3 °C and 5 °C were found by Cameron et al. (2014) and Djedjig et al. (2015), but in both studies the temperatures were measured significantly closer to the wall than in this research, at an 8 cm and 50 cm distance respectively. These outcomes suggest that the cooling effect of the green facade reduces as the distance from the wall increases, resulting in the facade greening having hardly any effect on the air temperature at a height of 1.4 meters and at 1 meter from the facade.

In contrast, green facades caused a larger decrease in surface temperature of the building walls (3-5 °C). The cooling effect of green facades on surface temperatures found in this study was with 2-6 °C comparable to that found in a German study (Bartfelder & Köhler, 1987), but less than the reported 10 °C for warmer climate (Alexandri & Jones, 2008; Hoelscher et al., 2016). Results of Ip et al. (2010) established a relationship between air temperature and surface temperature, where lower surface temperatures in the presence of a greened facade resulted in lower air temperature. Ip et al. (2010) explained this relationship by the correlation between the thickness and geometry of the leaf coverage and the amount of shortwave radiation that reached the facade through the leaves. The results of this study however show

that the effect of the reduced surface temperature in the presence of the greened facade on air temperature in front of the wall was negligible.

The orientation, on the other hand, led to larger air temperature differences (up to 2.4 °C) between the simulations with bare walls of the coldest north and hottest south model simulation. These differences occurred during daytime and were significantly smaller for the east and west oriented model simulations when compared to the southern orientation (< 1.0 °C). These temperature differences are consistent with the differences in shortwave radiation received by the wall, where a maximum difference of 600 to 750 W/m² was found between the northern and the southern orientation. Higher surface temperatures due to the larger amount of shortwave radiation received led to higher air temperatures in the street (Ali-Toudert & Mayer, 2007).

In conclusion, orientation leads to larger differences in local air temperature than the implementation of greened facades. Although green facades reduced the amount of shortwave radiation received by the wall and thus the surface temperatures, these effects were a lot smaller than the reduced amount of shortwave radiation received by a differently oriented facade in the first place.

Physiologically Effective Temperature (PET)

Building orientation appeared to have a larger impact on PET in front of building wall facade than facade greening. PET-differences of 8 °C between the north and south orientation models were obtained. Of all parameters affecting PET, especially the mean radiant temperature seemed to affect the outdoor thermal comfort. The mean radiant temperature is determined by the shortwave and longwave radiative fluxes and is the most dominant factor for the way people perceive thermal comfort (Mikler et al., 2009). The results showed a nearly identical pattern between the shortwave radiation received and the mean radiant temperature at the considered grid cells, suggesting that the shortwave radiation is a good indicator for T_{mrt} and eventually PET. This contradicts the outcome of research by A Matzarakis et al. (2003), whose results of linear regressions did indicate a strong relationship between PET and T_{mrt} (R2=0.746), but showed a relatively low effect of the received shortwave radiation. Hardly an effect of green facades on wind speed close to the wall surface was found. This is in agreement with Perini et al. (2011) who showed that green facades cause only a small extra reduction in wind speed (0.25 m/s) close to the wall surface. So, the small wind reducing effect of green facades hardly has an effect on PET. Again, the orientation of the facade has a larger influence depending on the wind direction.

The cooling effect of green facades on PET remained below a 0.7 °C cooling for all orientations, and sometimes even led to an increase in temperatures. Since the orientation could cause a distinction of two classes in the grade of physiological stress due to the large differences in T_{mrt} (e.g. between extreme heat stress, as experienced in the southern model, or moderate heat stress, which was felt in the northern model at the same time), this influence is more significant compared to the impact of the green facade, where no distinction in grade of physiological stress is noticeable.

6. 3. Indoor air temperature

The green facades significantly reduced the interior air temperature compared to the simulation with bare walls in the first three days. These differences mainly occurred during daytime and accumulated to 3 °C for the southern orientation, 2.5 °C for the east and west and 1.8 °C for the northern oriented study area. This is in line with the findings of Tilley et al. (2012) who showed that the cooling effect of six vine species over June, July and August in Maryland was most pronounced during the afternoon. The largest differences in interior air temperature correlated with the amount of shortwave radiation received and absorbed by the wall with and without a green facade. A 70 percent decrease in shortwave radiation received at the wall surface was obtained.

However, in the last two days of the simulation, the green facade caused interior temperature oscillations, showing higher interior temperatures at night and lower temperatures during the day than in the simulations with a bare wall. This seemed to be due to the insulating effect of the green facade which reduces the heat flux through the wall. At night the impact of the green facade is lower due to the absence of evapotranspiration and solar radiation. During the day, the green facade still provided cooling, because less heat entered through the facade due to the reduced absorption of shortwave radiation. This corresponded with results from Pan & Xiao (2014), indicating an increase in thermal resistance of the wall through the extra insulation layer. This increased insulation decreased the heat flux through the wall in both directions: it prevented heat coming into the buildings, but also reduced the outward heat flow. As the thermal resistance of the bare walls of the simulated buildings in this research was low (R =0.41 W/m2k, compared to the currently prescribed R = 3.5 W/m2k), the enhanced R-value as a result of the facade greening can explain the initial reduction and eventual increase of the inside temperature. Depending on the R-value of the building, the additional insulating effect of the green facade reduces as the R-value of the walls increases (Tilley et al., 2012). The implementation of green facades is thus most effective for buildings with low insulation.

Throughout the last simulation days, this insulating effect retained the slowly accumulated heat inside the building, resulting in higher interior temperatures during the night than without a green facade. These findings contradict the outcomes of Hoelscher et al. (2016) suggesting that facade greening mostly decreases interior temperatures during night-time. Their findings differ from results obtained in this thesis as the largest differences in their research occurred for an indirect greening system, leading to possible air circulation between the wall and greening at night. Besides, Hoelscher et al. (2016) performed measurements for a 4-day period in which the differences between the bare wall and green facade interior air temperatures decreased over the days. This suggests that the indirect green facades delay the interior heat accumulation of buildings, but eventually still function as an extra insulation layer.

The orientation of the building significantly influenced the indoor air temperature: a difference in maximum temperature of 7 °C was obtained between the western and northern oriented study areas. Deviations took place during the daytime, emphasizing the impact of shortwave radiation received by the dwellings on indoor temperature. The inclination of the sun and the amount of shortwave radiation transmitted through the windows had the largest impact on the interior air temperatures. Especially east and west-facing windows are exposed to larger amounts of solar radiation due to the position of the sun in summer (Rovers et al., 2014). This leads to larger amounts of solar radiation being transmitted through the window into the house after sunrise and before sunset, respectively.

Indoor air temperatures are evaluated throughout the entire building instead of one room due to the absence of compartmentation in the ENVI-met simulations. In real buildings the temperature is not the same for all rooms or floors, due to the transmissivity of light and solar radiation through the windows and heat flux through walls. Detailed results per room are currently not yet technically supported by ENVI-met, which may lead to incorrect assumptions about the effect on the indoor temperature.

Depending on the length of the heatwave, the results indicate that increased insulation can lead to higher indoor temperatures during the day. This in addition to the initial heatwave leads to unfavourable conditions in terms of heat stress. The insulating function of the green facade, however, can still provide cooling when either the building is prevented from heating up or there is sufficient ventilation to dissipate the heat obtained. Combining green facades with other measures provides multiple opportunities. First of all, this research does not include a ventilation strategy, which leads to retained heat in the building. Good ventilation late in the evening or early in the morning could provide a good opportunity to keep the interior temperatures low. Next, because of the delayed heat flux, the heating would be prevented. Another possibility suggested by Hoelscher et al. (2016) is the application of facades that can be oriented parallel to walls during the day to decrease the received shortwave radiation, and perpendicular at night to increase the airflow and decrease the level of insulation, allowing better cooling during the night. Finally, it could be prevented that buildings have windows facing east or west, to prevent a lot of solar radiation coming in through the windows. If the buildings are oriented as such, sunscreens could stop the incoming solar radiation, to prevent heating.

It is clear that higher insulation values can be counterproductive and keep homes warmer. Green facades could reduce the energy consumption of buildings in both summer and winter. The most obvious is the reduction in heat loss in winter because the heat flux through the wall is reduced. Because of the expected increase in the number of tropical days and nights as predicted by KNMI (2015), it is expected that more Dutch citizens will utilize air conditioners in the future to cool their houses. Several studies show that green facades can significantly reduce peak cooling requirements due to the increased insulation (Alexandri & Jones, 2008). The effectiveness depends on outside air temperatures, types of green facades, orientation and (other) insulation of the buildings.

7. CONCLUSION

This thesis reports on simulations studies on the impact of green facades in combination with building orientation on outdoor thermal comfort in areas adjacent to buildings and on temperatures inside buildings. The focus was on dwellings of housing corporations in the city of Amsterdam that are poorly insulated and located in neighbourhoods that were most exposed to heat. The underlying study showed that green facades could potentially make a significant impact when implemented on these dwellings.

The presence of the green facade only resulted in outdoor temperature differences smaller than 1°C, which is barely perceptible by humans. In contrast, the orientation of buildings could account for differences of more than one physiological stress class (roughly 8 °C) of thermal comfort. Especially the received shortwave radiation proved to influence PET. The largest decrease in air temperature in the presence of a green facade was found in front of dwellings in the hottest orientation.

The highest indoor and outdoor temperatures were obtained at different orientations: sunshine entering through the windows resulted in the highest air temperatures inside the west-oriented buildings, while the largest outdoor heat stress occurred in front of the south-oriented facade, where the facade received the largest amount of shortwave radiation. By reducing the amount of absorbed shortwave radiation and increasing insulation, the green facade provided the greatest cooling indoors for buildings with a south orientation. Green facades decreased the amount of shortwave radiation reaching the wall surfaces. In all orientations, green facades caused a similar decrease in the amount of shortwave radiation reaching the wall. Because the southern orientation received the largest amount of shortwave radiation, the presence of the green facade provided the greatest cooling for this orientation. During the entire heatwave, regardless of the presence of green facades, the lowest indoor and outdoor temperatures were obtained in the north-oriented study area.

During the investigated heatwave the increased insulation by the facade greening initially slowed down the heat accumulation of the buildings. In the course of the heatwave, nevertheless, the green facades caused lower temperatures in the night, but higher temperatures during the day than without the green facade. To achieve low indoor temperatures both during the day and night, green facades would be best implemented in combination with other measures such as ventilation or shading mechanisms.

This study shows that further research into green facades in combination with other measures is important to be able to make well-founded policy choices for existing dwellings of housing corporations that are poorly insulated and are located at urban hot spots.

8. RECOMMENDATIONS

This thesis focuses on the effect of green facades on thermal comfort indoors as well as outdoors in urban areas exposed to heat. To further broaden the knowledge on green facades research topics are suggested that warrant further investigation. In addition, suggestions for practical implementation have also been formulated for urban planners, housing corporations, municipalities and other parties such as homeowners that consider using green facades as a climate adaptation measure.

Future research

For a more comprehensive image of critical hot zones indoors and outdoors, a combination of UHI, PET and energy label maps is suggested. This corresponds to the Standard Heat Stress Test as developed by Rijksinstituut voor Volksgezondheid en Milieu (RIVM) (2019). To identify the most exposed heat areas in Amsterdam, the UHI was used in this research, since high temperatures reached during heatwaves are often exacerbated due to the UHI. The UHI indicated the most critical heat areas in the city independent of human perception. Although the use of UHI has drawbacks as it mainly reflects the difference between urban and rural areas and especially influences temperatures at night and not during the day, it is currently the best way to reflect exposure. The combination of the suggested indicators could be used for a more comprehensive impression of the problematic heat areas in the city.

Further research into ways to maximise the effect of the greened facades is important. The results of this research demonstrate that green facades can function as a mitigation strategy to reduce heat issues. To optimize heat reduction taking into account the heat accumulation during heatwaves, green facades could, for example, be used in combination with other cooling strategies, such as sun blinds or different ventilation mechanisms. By experimenting with different compositions, the maximum cooling effect of green walls could be achieved. In addition, H. helix was used in this study in the form of a direct green facade as it is a common species in Western Europe and it is incorporated in the ENVI-met database. However, as Hoelscher et al. (2016) pointed out, different types of green facades could provide for different cooling effects. Furthermore, it would be of considerable interest to investigate the effect of different species. Cameron et al. (2014) and Tilley et al. (2012) identified that the cooling effect of green facades differs significantly among species by shading, evaporation rate and leaf area index. A comparative study of direct and indirect green facades and different species is thus suggested to identify the best cooling type of green facade.

The results of this study illustrate that the cooling effect of green facades changes considerably the longer the heatwave lasts. In this study a heatwave of five consecutive

days was investigated, but for a more comprehensive picture of the heat accumulation in buildings, it is recommended to perform simulations for longer periods. Likewise, it is advised to undertake a sensitivity analysis that examines the effect of green facades on buildings with both higher and lower insulation values to pinpoint on which buildings implementation would be most effective.

Throughout this research the thermal comfort has been studied from a physical perspective, with a focus on meteorological and human-biometeorological indices such as air temperature and PET. The perceived thermal comfort was not addressed here. Klemm et al. (2015) demonstrated that green infrastructure improves perceived thermal comfort. In tackling the heat problem, it is therefore meaningful to include these psychological effects of facade greening on heat perception. By linking air temperature, PET and the psychological effects in a model and experimental setup, more knowledge could be gathered in this subject.

The obtained results suggest that green facades can function as an extra insulation layer of walls. Given the insulating value, it is urgent to simulate the effect of green facades for other seasons and particularly in winter. The insulating value, for example, has not yet been linked in this research to an energy reduction or cost reduction. Linking the effect of green facades to energy consumption and investigating this during both hot and cold periods could provide a more comprehensive picture of the insulating effect in the Dutch climate. Also, a cost-benefit analysis or multi-criteria analysis comparing green facades with classic insulation mechanisms would contribute to current knowledge. Moreover, further research could fortify well-founded policy decisions for existing dwellings of housing corporations that are poorly insulated.

Ensuring the use of green facades as a cooling mechanism, it is of great necessity that research is additionally carried out into implementation in the local climate. Several factors need to be considered. For example, due to the building orientation and surrounding urban microclimate, the facade greening can be subject to extreme temperature fluctuations (hot during the days and cold during nights), wind speed differences and sunlight exposure. Different species function better on different oriented walls due to their characteristics in combination with the extreme variation in temperatures (Atelier GROENBLAUW, n.d.). Furthermore, the cooling capabilities of H. helix are based on a fully grown plant. As it takes up to 3-5 years to cover the whole façade, the cooling effects will initially not be very significant. In addition the use of H. helix is often linked to damaged facades due to its strong root that is difficult to remove (FassadenGrün, 2020). These issues generally don't arise on flat walls without cracks. When installing green facades, it is thus important to take into account the buildings' characteristics, characteristics of different species and the local climate to compose the best combination.

Furthermore, beyond the effects on the inside and outside thermal comfort, green facades are known for having various co-benefits on the city environment. Implementing green facades can lower greenhouse gas emissions, improve air quality, creating habitats for several urban species and lowering noise in the surrounding areas (Besir & Cuce, 2018; Currie & Bass, 2008; Köhler, 2008; Lundholm, 2006). By combining these aspects and researching the green facade performance, ecosystem service valuation, design parameters and practical management of the growth of the species the overarching positive impacts and limitations of green facades on the local climate can be assessed.

Suggestions for practical implementation

Based on this research, the following advice can be formulated for municipalities, housing corporations, urban planners and designers, but also for citizens who would like to install their own green facade to improve the thermal comfort in and around their homes:

- To find out where heat problems are greatest in the city, it is recommended for public authorities to create heat exposure maps and keep such maps up to date. Such information is crucial to make well-informed policy decisions on the application of green facades.
- As building orientation proved to significantly affect outdoor and indoor thermal comfort, public authorities in their housing policy decision making are advised to minimize the amount of west (and to a lesser extend east) oriented buildings if possible.
- When west or east oriented buildings are constructed after all, it is important to minimise the number of windows on these facades, if any, or at least to make them as small as feasible to prevent solar heating
- Green facades could be used as an additional insulation mechanism to prevent heat accumulation of dwellings. Depending on the cooling need, it could be applied in combination with other strategies
- The outdoor local effect of green facades on thermal comfort is small but could be applied in combination with other heat mitigation strategies
- For east and west oriented buildings (green) shading mechanisms could be beneficial to reduce the heat transfer through windows
- Public authorities are recommended to develop clear guidance regarding possible benefits of green facades and thereby stimulate homeowners and housing corporations to consider green facades.

9. LITERATURE

Alexandri, E., & Jones, P. (2004). The thermal effects of green roofs and green façades on an urban canyon. The 21th Conference on Passive and Low Energy Architecture. Eindhoven, The Netherlands.

Alexandri, E., & Jones, P. (2008). Temperature decreases in an urban canyon due to green walls and green roofs in diverse climates. Building and Environment, 43(4), 480–493.

Ali-Toudert, F., & Mayer, H. (2007). Thermal comfort in an east–west oriented street canyon in Freiburg (Germany) under hot summer conditions. Theoretical and Applied Climatology, 87(1–4), 223–237.

Andersson, B., Place, W., Kammerud, R., & Scofield, M. P. (1985). The impact of building orientation on residential heating and cooling. Energy and Buildings, 8(3), 205–224.

Atelier GROENBLAUW. (n.d.). Urban green-blue grids: green facades. https://nl.urbangreenbluegrids.com/measures/green-facades/

Barriopedro, D., Fischer, E. M., Luterbacher, J., Trigo, R. M., & García-Herrera, R. (2011). The hot summer of 2010: redrawing the temperature record map of Europe. Science, 332(6026), 220–224.

Bartfelder, F., & Köhler, M. (1987). Experimentelle Untersuchungen zur Funktion von Fassadenbegrünungen. A (1987). Berlin-Verlag.

Berry, R., Livesley, S. J., & Aye, L. (2013). Tree canopy shade impacts on solar irradiance received by building walls and their surface temperature. Building and Environment, 69, 91–100.

Besir, A. B., & Cuce, E. (2018). Green roofs and facades: A comprehensive review. Renewable and Sustainable Energy Reviews, 82, 915–939.

Birkmann, J. (2006). Measuring vulnerability to promote disaster-resilient societies: Conceptual frameworks and definitions. Measuring Vulnerability to Natural Hazards: Towards Disaster Resilient Societies, 1, 9–54.

Bruse, D. (2018). Winter release: ENVI-met V4.4. https://www.envi-met.com/winter-release-envi-met-v4-4/

Bruse, M. (2000). Die Auswirkungen kleinskaliger Umweltgestaltung auf das Mikroklima.

Bruse, M., & Fleer, H. (1998). Simulating surface-plant-air interactions inside urban environments with a three dimensional numerical model. Environmental Modelling and Software, 13(3–4), 373–384. https://doi.org/10.1016/S1364-8152(98)00042-5

Building Archive Municipality of Amsterdam. (2020). Saffierstraat 13 Zuid. 09-01-2020

Cameron, R. W. F., Taylor, J. E., & Emmett, M. R. (2014). What's 'cool'in the world of green façades? How plant choice influences the cooling properties of green walls. Building and Environment, 73, 198–207.

Cardona, O. D. (2011). Disaster risk and vulnerability: Concepts and measurement of human and environmental insecurity. In Coping with global environmental change, disasters and security (pp. 107–121). Springer.

Currie, B. A., & Bass, B. (2008). Estimates of air pollution mitigation with green plants and green roofs using the UFORE model. Urban Ecosystems, 11(4), 409–422.

Dirksen, M., Ronda, R. J., Theeuwes, N. E., & Pagani, G. A. (2019). Sky view factor calculations and its application in urban heat island studies. Urban Climate, 30, 100498.

Djedjig, R., Bozonnet, E., & Belarbi, R. (2015). Experimental study of the urban microclimate mitigation potential of green roofs and green walls in street canyons. International Journal of Low-Carbon Technologies, 10(1), 34–44.

FassadenGrün. (2020). Hedera helix (general Ivy). https://www.fassadengruen.de/en/english-ivy.html

Francis, R. A., & Lorimer, J. (2011). Urban reconciliation ecology: the potential of living roofs and walls. Journal of Environmental Management, 92(6), 1429–1437.

Gemeente Amsterdam. (2016). Beleidskader voor het toetsen van ingrepen of herstel van monumenten.

Gemeente Amsterdam West. (2014). Plan Openbare Ruimte Frederik Hendrikbuurt. https://www.amsterdam.nl/projecten/frederik/

Gross, G. (2012). Effects of different vegetation on temperature in an urban building environment. Micro-scale numerical experiments. Meteorologische Zeitschrift, 21(4), 399–412.

Hoelscher, M.-T., Nehls, T., Jänicke, B., & Wessolek, G. (2016). Quantifying cooling effects of facade greening: Shading, transpiration and insulation. Energy and Buildings, 114, 283–290.

Höppe, P. (1999). The physiological equivalent temperature–a universal index for the biometeorological assessment of the thermal environment. International Journal of Biometeorology, 43(2), 71–75.

Huurcommissie. (2019). Beleidsboek waarderingsstelsel zelfstandige woonruimte.

Ip, K., Lam, M., & Miller, A. (2010). Shading performance of a vertical deciduous climbing plant canopy. Building and Environment, 45(1), 81–88.

IPCC. (2012). Managing the risks of extreme events and disasters to advance climate change adaptation: special report of the intergovernmental panel on climate change. Cambridge University Press.

IPCC. (2013). Climate Change 2013: The physical science basis. contribution of working group I to the fifth assessment report of IPCC the intergovernmental panel on climate change (T. F. Stocker, D. Qin, G.-K. Plattner, M. M. B. Tignor, S. K. Allen, J. Boschung, A. Nauels, Y. Xia, V. Bex, & P. M. Midgley (eds.)). Cambridge University Press.

ISSO. (2009). Formula Structure Publicatie 82.3 Handleiding EPA-W (Formulestructuur). Senternovem, 82(3).

Jänicke, B., Meier, F., Hoelscher, M. T., & Scherer, D. (2015). Evaluating the effects of façade greening on human bioclimate in a complex Urban environment. Advances in Meteorology, 2015. https://doi.org/10.1155/2015/747259

Janssen, M. A., Schoon, M. L., Ke, W., & Börner, K. (2006). Scholarly networks on resilience, vulnerability and adaptation within the human dimensions of global environmental change. Global Environmental Change, 16(3), 240–252.

Kenney, W. L., Craighead, D. H., & Alexander, L. M. (2014). Heat waves, aging, and human cardiovascular health. Medicine and Science in Sports and Exercise, 46(10), 1891.

Kleerekoper, L. (2017). Urban Climate Design: Improving thermal comfort in Dutch neighbourhoods. A+ BE| Architecture and the Built Environment, 11, 1–424.

Klemm, W., Heusinkveld, B. G., Lenzholzer, S., Jacobs, M. H., & Van Hove, B. (2015). Psychological and physical impact of urban green spaces on outdoor thermal comfort during summertime in The Netherlands. Building and Environment, 83, 120–128.

Klok, L., & Kluck, J. J. (2018). Reasons to adapt to urban heat (in the Netherlands). Urban Climate, 23, 342–351.

Klok, L., Rood, N., Kluck, J., & Kleerekoper, L. (2019). Assessment of thermally comfortable urban spaces in Amsterdam during hot summer days. International Journal of Biometeorology, 63(2), 129–141.

Kluck, J., Klok, L., Solcerov, A., Kleerekoper, L., Wilschut, L., & Jacobs, C. (2020). De hittebestendige stad. Onderzoeksprogramma Urban Technology, Faculteit Techniek, Hogeschool van Amsterdam.

KNMI. (2015). KNMI'14-klimaatscenario's voor Nederland; Leidraad voor professionals in klimaatadaptatie. http://www.klimaatscenarios.nl/images/Brochure_KNMI14_NL.pdf

Köhler, M. (2008). Green facades—a view back and some visions. Urban Ecosystems, 11(4), 423.

Kort, E. (2009). Lambda waarde materialen. Omgevingsvergunning.Com. http://www.ekbouwadvies.nl/tabellen/lambdamaterialen.asp

Krusche, P., von Lersner, H., & Otto, K. (1982). Ökologisches bauen. Springer.

Lauwaet, D., Hooyberghs, H., Maiheu, B., Lefebvre, W., Driesen, G., Van Looy, S., & De Ridder, K. (2015). Detailed urban heat island projections for cities worldwide: dynamical downscaling CMIP5 global climate models. Climate, 3(2), 391–415.

Lin, T.-P., & Matzarakis, A. (2008). Tourism climate and thermal comfort in Sun Moon Lake, Taiwan. International Journal of Biometeorology, 52(4), 281–290.

Lundholm, J. T. (2006). Green roofs and facades: a habitat template approach. Urban Habitats, 4(1), 87–101.

Majcen, D., Itard, L. C. M., & Visscher, H. (2013). Theoretical vs. actual energy consumption of labelled dwellings in the Netherlands: Discrepancies and policy implications. Energy Policy, 54, 125–136.

Matzarakis, A, Mayer, H., & Rutz, F. (2003). Radiation and thermal comfort. Proceeding of 6th Hellenic Conference in Meteorology, Climatology and Atmospheric Physics.

Matzarakis, Andreas, & Mayer, H. (1996). Another kind of environmental stress: thermal stress. WHO Newsletter, 18(January 1996), 7–10.

Mikler, V., Bicol, A., Breisness, B., & Labrie, M. (2009). Passive Design Toolkit. Vancouver, City of Vancouver.

Ministerie van Volkshuisvesting en Ruimtelijke Ordening. (1969). Voorschriften en wenken voor het ontwerpen van woningen (1965). LK - (4e dr.). Staatsuitgeverij. https://tudelft.on.worldcat.org/oclc/841087293

Molenaar, R. E., Heusinkveld, B. G., & Steeneveld, G. J. (2016). Projection of rural and urban human thermal comfort in The Netherlands for 2050. International Journal of Climatology, 36(4), 1708–1723.

Nguyen, J. L., Schwartz, J., & Dockery, D. W. (2014). The relationship between indoor and outdoor temperature, apparent temperature, relative humidity, and absolute humidity. Indoor Air, 24(1), 103–112.

Oke, T. R. (1976). The distinction between canopy and boundary layer urban heat islands. Atmosphere, 14(4), 268–277.

Oke, T. R. (1982). The energetic basis of the urban heat island. Quarterly Journal of the Royal Meteorological Society, 108, 1–24.

Oke, T. R. (1988). The urban energy balance. Progress in Physical Geography, 12(4), 471–508.

Ostendorf, M., Retzlaff, W., Thompson, K., Woolbright, M., Morgan, S., & Celik, S. (2011). Storm water runoff from green retaining wall systems. Cities Alive!: Ninth Annual Green Roof and Wall Conference, 1–15.

Ottelé, M. (2011). The green building envelope. Vertical greening [Ph. D. thesis]. Delft University of Technology.

Pan, X. C., & Xiao, Y. X. (2014). Simulation analysis of building green facade eco-effect. Applied Mechanics and Materials, 548, 1701–1705.

Peck, S. W., Callaghan, C., Kuhn, M. E., & Bass, B. (1999). Greenbacks from green roofs: forging a new industry in Canada. Citeseer.

Peng, S., Piao, S., Ciais, P., Friedlingstein, P., Ottle, C., Bréon, F.-M., Nan, H., Zhou, L., & Myneni, R. B. (2012). Surface urban heat island across 419 global big cities. Environmental Science & Technology, 46(2), 696–703.

Perez, G., Rincon, L., Vila, A., Gonzalez, J. M., & Cabeza, L. F. (2011). Green vertical systems for buildings as passive systems for energy savings. Applied Energy, 88(12), 4854–4859.

Perini, K., Ottelé, M., Fraaij, A. L. A., Haas, E. M., & Raiteri, R. (2011). Vertical greening systems and the effect on air flow and temperature on the building envelope. Building and Environment, 46(11), 2287–2294.

Perini, K., & Rosasco, P. (2013). Cost–benefit analysis for green façades and living wall systems. Building and Environment, 70, 110–121.

Piringer, M., Grimmond, C., Joffre, S., Mestayer, P., Middleton, D., Rotach, M., Baklanov, A., De Ridder, K., Ferreira, J., Guilloteau, E., Karppinen, A., Martilli, A., Masson, V., & Tombrou, M. (2002). Investigating the Surface Energy Budget in Urban Areas - Recent Advances and Future Needs. Water, Air, & Soil Pollution: Focus, 2, 1–16. https://doi.org/10.1023/A:1021302824331

Quinn, A., Tamerius, J. D., Perzanowski, M., Jacobson, J. S., Goldstein, I., Acosta, L., & Shaman, J. (2014). Predicting indoor heat exposure risk during extreme heat events. Science of the Total Environment, 490, 686–693.

Rijksinstituut voor Volksgezondheid en Milieu (RIVM). (2019). Development of a Standard Heat Stress Test.

RIVM. (2018). Stedelijk hitte-eiland effect (UHI) in Nederland. Atlas Natuurlijk Kapitaal. http://nationaalgeoregister.nl/geonetwork/srv/dut/catalog.search#/metadata/a87f5ca8-f354-4ff6-adc3-70f1bf6b78e3?tab=general

Rovers, V., Bosch, P., Albers, R., & Spit, T. (2014). Climate proof cities. TNO.

Runhaar, H., Mees, H., Wardekker, A., van der Sluijs, J., & Driessen, P. P. J. (2012). Adaptation to climate change-related risks in Dutch urban areas: stimuli and barriers. Regional Environmental Change, 12(4), 777–790.

Sadineni, S. B., Madala, S., & Boehm, R. F. (2011). Passive building energy savings: A review of building envelope components. Renewable and Sustainable Energy Reviews, 15(8), 3617–3631.

Skelhorn, C., Lindley, S., & Levermore, G. (2014). The impact of vegetation types on air and surface temperatures in a temperate city: A fine scale assessment in Manchester, UK. Landscape and Urban Planning, 121, 129–140. https://doi.org/10.1016/j.landurbplan.2013.09.012

Sociaal-Economische Raad. (2013). Energieakkoord voor duurzame groei (Issue September).

Taha, H. (1997). Urban climates and heat islands: Albedo, evapotranspiration, and anthropogenic heat. Energy and Buildings, 25(2), 99–103.

Taleghani, M., Tenpierik, M., & van den Dobbelsteen, A. (2014). Indoor thermal comfort in urban courtyard block dwellings in the Netherlands. Building and Environment, 82, 566–579.

Tamerius, J. D., Perzanowski, M. S., Acosta, L. M., Jacobson, J. S., Goldstein, I. F., Quinn, J. W., Rundle, A. G., & Shaman, J. (2013). Socioeconomic and outdoor meteorological determinants of indoor temperature and humidity in New York City dwellings. Weather, Climate, and Society, 5(2), 168–179.

Tilley, D., Price, J., Matt, S., & Marrow, B. (2012). Vegetated walls: thermal and growth properties of structured green facades. Final Report to Green Roofs for Healthy Cities.

UNISDR. (2004). Reducing Disaster Risk: A Challenge for Development-a Global Report. United Nations International Strategy for Disaster Reduction of Extreme Events and Disasters to Advance Climate Change Adaptation : Special Report of the Intergovernmental Panel on Climate Change. Cambridge University Press.

van Hooff, T., Blocken, B., Hensen, J. L. M., & Timmermans, H. J. P. (2014). On the predicted effectiveness of climate adaptation measures for residential buildings. Building and Environment, 82, 300–316.

Van Hove, L. W. A., Steeneveld, G. J., Jacobs, C. M. J., Heusinkveld, B. G., Elbers, J. A., Moors, E. J., & Holtslag, A. A. M. (2011). Exploring the urban heat island intensity of Dutch cities: assessment based on a literature review, recent meteorological observation and datasets provide by hobby meteorologists. Alterra.

Wilschut, L., Kleerekoper, L., & Kluck, J. (2019). Maak je stad hittebestendig met looptijd-tot-koelte kaarten. https://www.biind.nl/content/maak-je-stad-hittebestendig-met-looptijd-tot-koelte-kaarten

10. APPENDIX

A. Simulation input and output

To facilitate the reproduction process of this study, all input and output data of the model simulations is available via florindevessies.github.io/greenfacades.

B. Data requirements for Monde

The techniques used for data collection and the data requirement analysis for the simulations are described below.

Type of info	Description	Availability	Source	Pre-processing needed	Used in model
Buildings	All buildings in the neighbourhood	Need to be combined with heights from AHN (AHN3_0.5m_DTM)	Geofabrik.de	Yes, in ArcGIS Pro.	Grid of neighbourhood with maximum building heights, with brick stones as materials
Elevation models	Digital Terrain Model (DTM)	Available via PDOK	Pdok.nl	Yes, in ArcGIS Pro	Added to buildings
	Digital Surface Model	Available via PDOK	Pdok.nl	Yes, in ArcGIS Pro (to create actual heights of buildings)	no
Streets	All streets in the area		BGT Nederland		Combined with pavement. ENVI-met Pavement (concrete), used/dirty
Pavement	Location, width and size of pavement		BGT Nederland		Yes, but combined with streets
Soil type	Soil profile of the Diamantbuurt	Available up until 45 m below NAP. Upper layer is anthropogenic, followed by peat.	Dinoloket.nl		Sandy loam (needed for plants)
Vegetation	The location of vegetation areas such as gardens		BGT Nederland		Yes, as basic grass
Trees	All trees owned by the municipality	Maps.amsterdam.nl	Maps.amsterdam.nl		Spherical, medium trunk, low LAD, 5 m trees
Land use			Geofabrik.de		Not used in model